Compact Stars

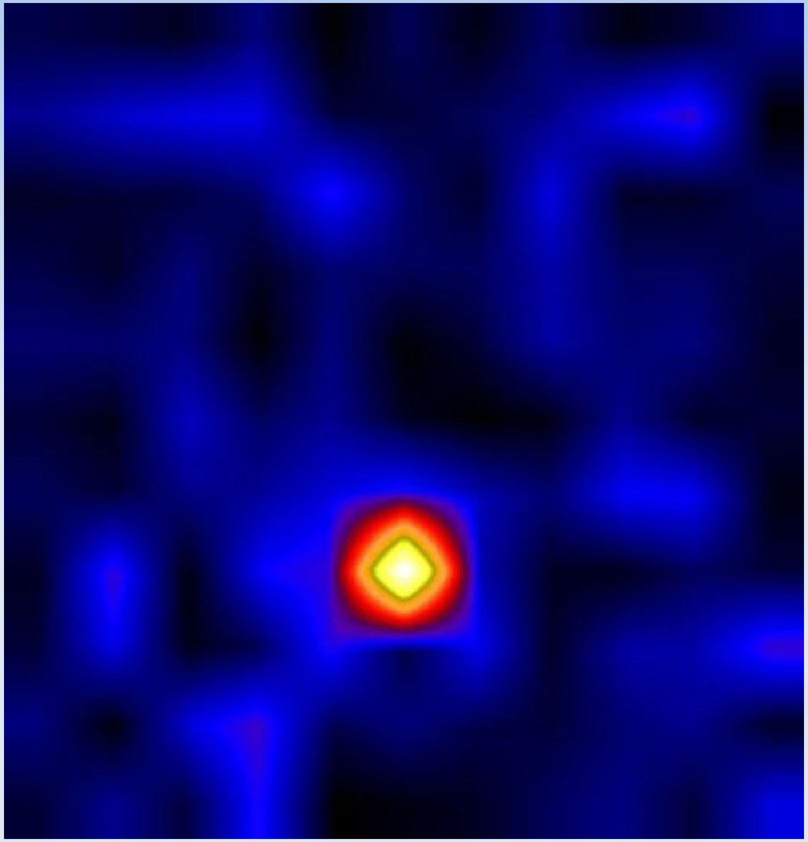

Lecture 5

Summary of the previous lecture

- We talked about the observed properties of X-ray binaries and the black body emission of accretion disk, plus the hard X-ray emission with power-law tail.
- I presented the milestones of X-ray astronomy history, and observational techniques used in X-ray domain.
- The classification of high and low mass X-ray binaries was supplemented with the evolutionary history of these systems.

X-ray spectral components

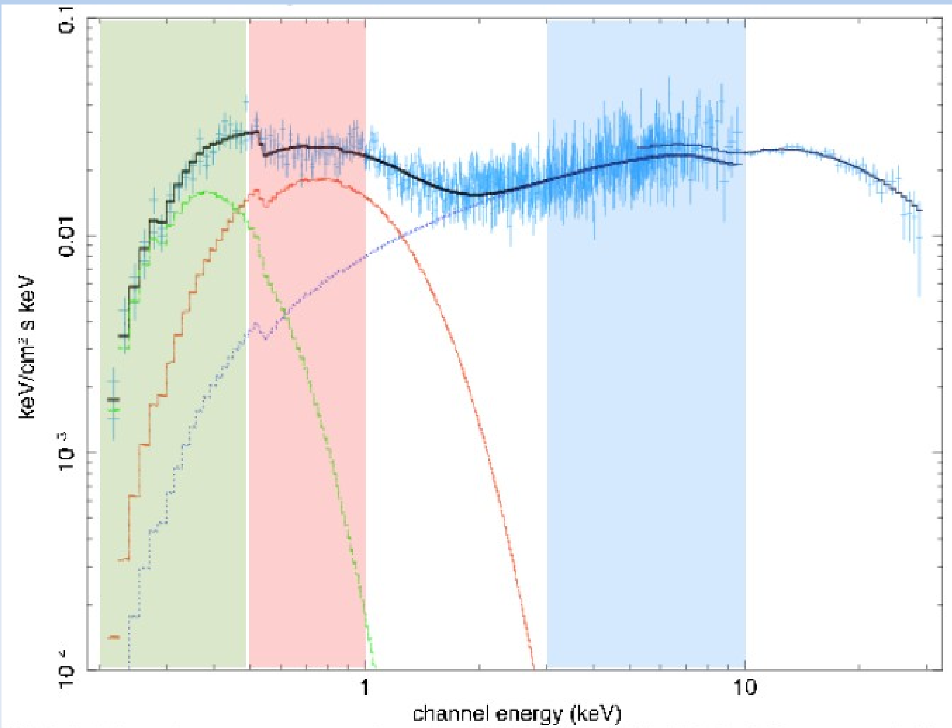

In August 2007, the X-ray binary pulsar XMMU J054134.7-682550 made a giant type II outburst, reaching the Eddington limit. The reflection of the hard X-ray, emitted close to the neutron star, on the inner part of the accretion disk allowed the determination of the geometry of the broadened inner disk (width of 75 km). The thermal emission from the disk could also be detected during the outburst. (e.g. Manousakis et al. 2009)

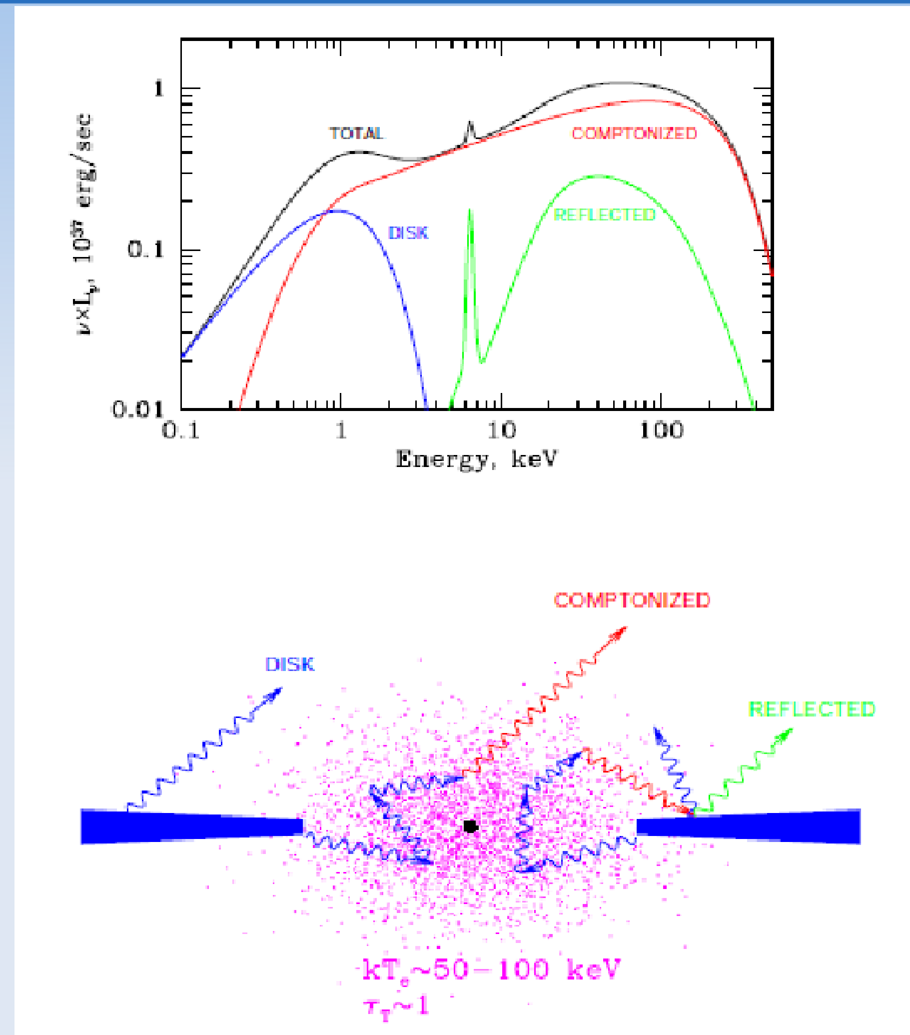

Three main components of the X-ray emission from an accreting black hole (top) and a plausible geometry of the accretion flow in the hard spectral state (bottom), from Gilfanov (2010)

Eddington limit

- Infalling matter is ionized hydrogen
- The upward force is exerted by the radiation flux, due to the Thomson scatterig on electrons

$$F_x = \frac{L_x \sigma_T}{4\pi r^2 c}$$

which is the number of collinsions per electron per unit time ($\sigma_T = 0.66 \times 10^{-24}$ cm^2), multiplied by photon momentum *p*

- These electrons communicate with protons by electrostatic coupling

Eddington limit

- Accretion occurs if the gravity exceeds the photon force.

$$F_{grav} = \frac{G M_X m_p}{r^2}$$

- The critical luminosity is therefore

$$L_{Edd} = \frac{4\pi G M_x m_p}{\sigma_T} = 1.3\times 10^{38} \left(\frac{M_X}{M_{Sun}}\right) erg\ s^{-1}$$

  and is called Eddington limit (Eddington 1926)

- The same limit applies to massive stars supported in hydrostatic equilibrium by radiation pressure

Today: disk instabilities, time-dependent accretion

- Today I will discuss the observations of Dwarf Nova outbursts as an example of accretion disk instability.
- I will show the formalism for time-dependent accretion disk models.
- The thermal and viscous instability of accretion disk will be described, based on the alpha-disk theory.

Novae

- Rate: 10/year
- Nacked eye events: 3-5 per century
- Thermonuclear explosion on WD star

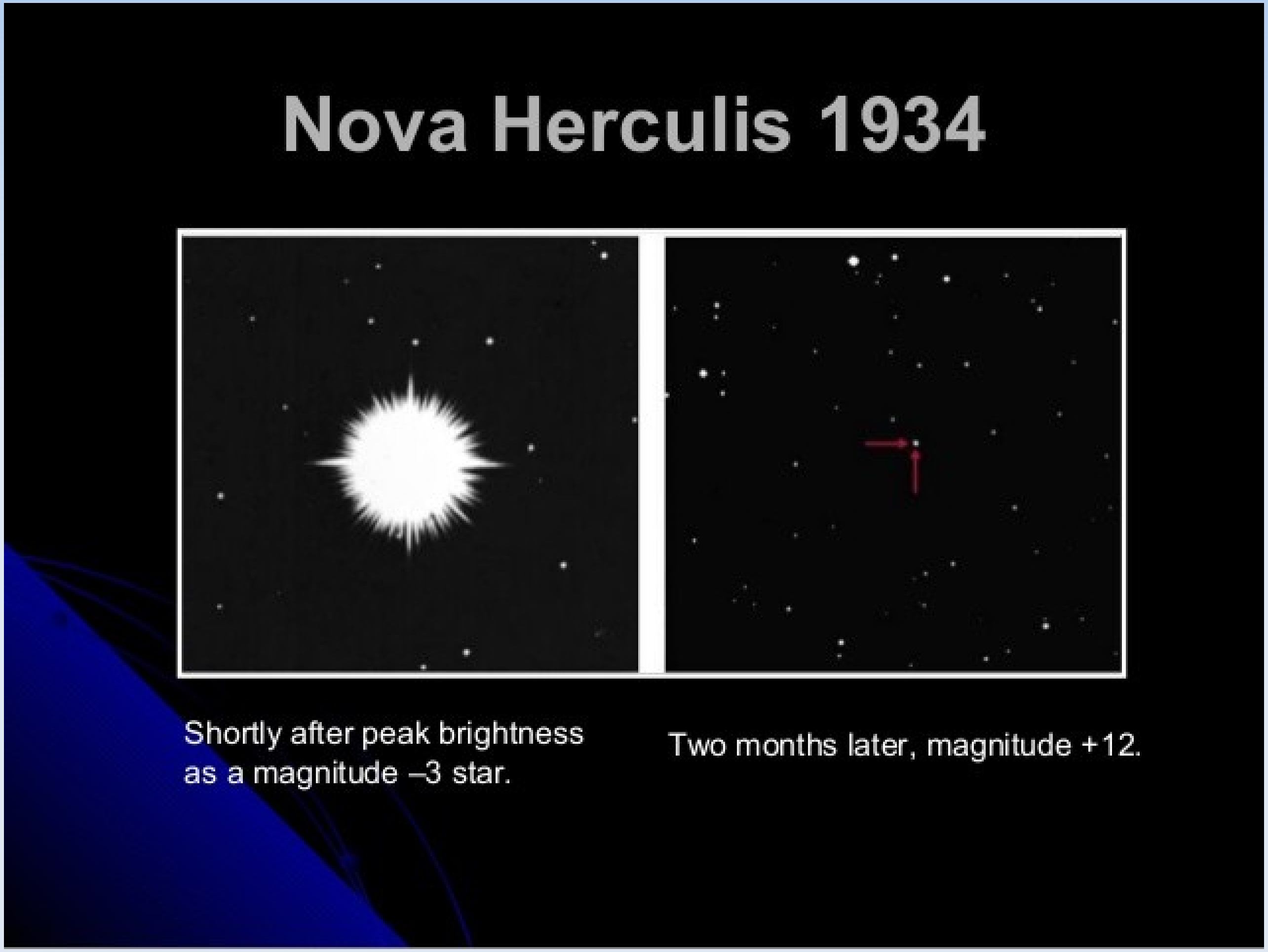

Binary system consisting of awhite dwarf primary with an estimated 60% of the massof the Sun and a redc dwarf secondary with 40% of the Sun's mass.

Classical Novae

- Nova eruption occurs due to hydrogen accumulation on the surface of white dwarf
- When temperature and density grows, runaway nuclear fusion starts (C-N-O cycle)

V1500 Cygni, occured in 1975. Brightened by 14 magnitudes, remained visible to the nacked eye for about a week. The WD has a strong magnetic field, preventing formation of an accretion disk (Semeniuk et al. 1977)

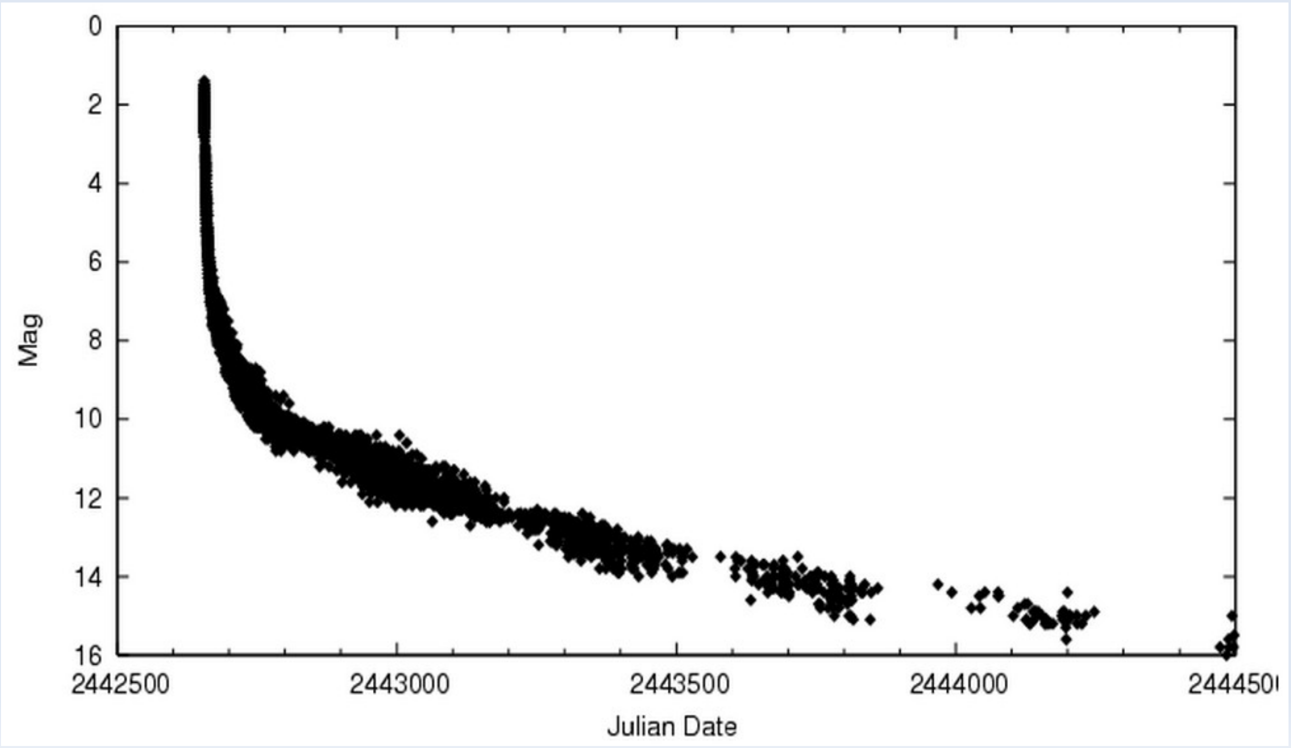

Nova Aquilae

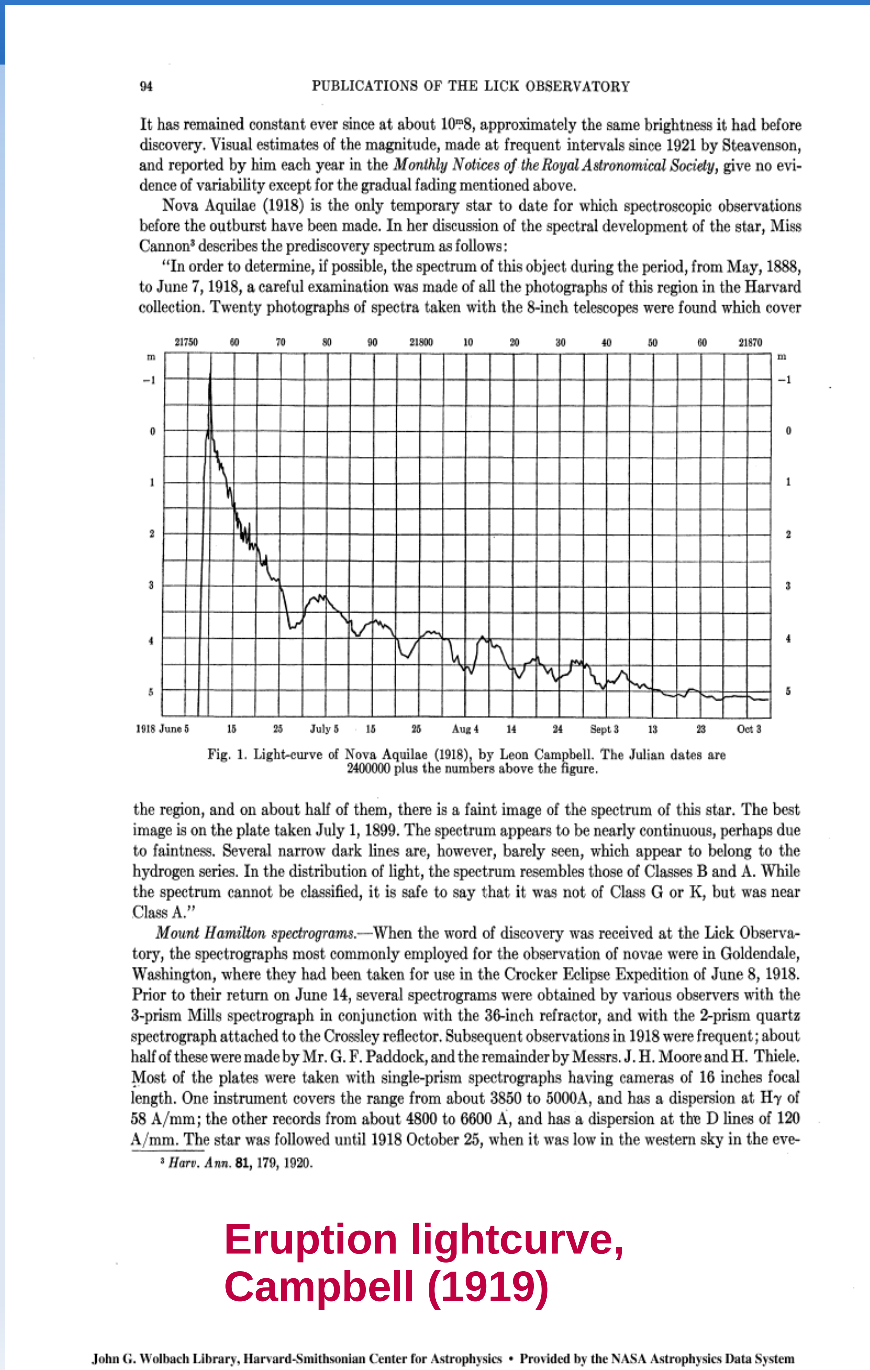

94 PUBLICATIONS OF THE LICK OBSERVATORY

It has remained constant ever since at about $10^m.8$, approximately the same brightness it had before discovery. Visual estimates of the magnitude, made at frequent intervals since 1921 by Steavenson, and reported by him each year in the *Monthly Notices of the Royal Astronomical Society*, give no evidence of variability except for the gradual fading mentioned above.

Nova Aquilae (1918) is the only temporary star to date for which spectroscopic observations before the outburst have been made. In her discussion of the spectral development of the star, Miss Cannon[3] describes the prediscovery spectrum as follows:

"In order to determine, if possible, the spectrum of this object during the period, from May, 1888, to June 7, 1918, a careful examination was made of all the photographs of this region in the Harvard collection. Twenty photographs of spectra taken with the 8-inch telescopes were found which cover the region, and on about half of them, there is a faint image of the spectrum of this star. The best image is on the plate taken July 1, 1899. The spectrum appears to be nearly continuous, perhaps due to faintness. Several narrow dark lines are, however, barely seen, which appear to belong to the hydrogen series. In the distribution of light, the spectrum resembles those of Classes B and A. While the spectrum cannot be classified, it is safe to say that it was not of Class G or K, but was near Class A."

Fig. 1. Light-curve of Nova Aquilae (1918), by Leon Campbell. The Julian dates are 2400000 plus the numbers above the figure.

Mount Hamilton spectrograms.—When the word of discovery was received at the Lick Observatory, the spectrographs most commonly employed for the observation of novae were in Goldendale, Washington, where they had been taken for use in the Crocker Eclipse Expedition of June 8, 1918. Prior to their return on June 14, several spectrograms were obtained by various observers with the 3-prism Mills spectrograph in conjunction with the 36-inch refractor, and with the 2-prism quartz spectrograph attached to the Crossley reflector. Subsequent observations in 1918 were frequent; about half of these were made by Mr. G. F. Paddock, and the remainder by Messrs. J. H. Moore and H. Thiele. Most of the plates were taken with single-prism spectrographs having cameras of 16 inches focal length. One instrument covers the range from about 3850 to 5000A, and has a dispersion at $H\gamma$ of 58 A/mm; the other records from about 4800 to 6600 A, and has a dispersion at the D lines of 120 A/mm. The star was followed until 1918 October 25, when it was low in the western sky in the eve-

[3] *Harv. Ann.* **81**, 179, 1920.

Eruption lightcurve, Campbell (1919)

V603 Aquilae (or Nova Aquilae 1918) was a bright nova first observed (from Earth) in the constellation Aquila in 1918. It was the brightest "new star" to appear in the sky since the Kepler's Supernova in 1604.

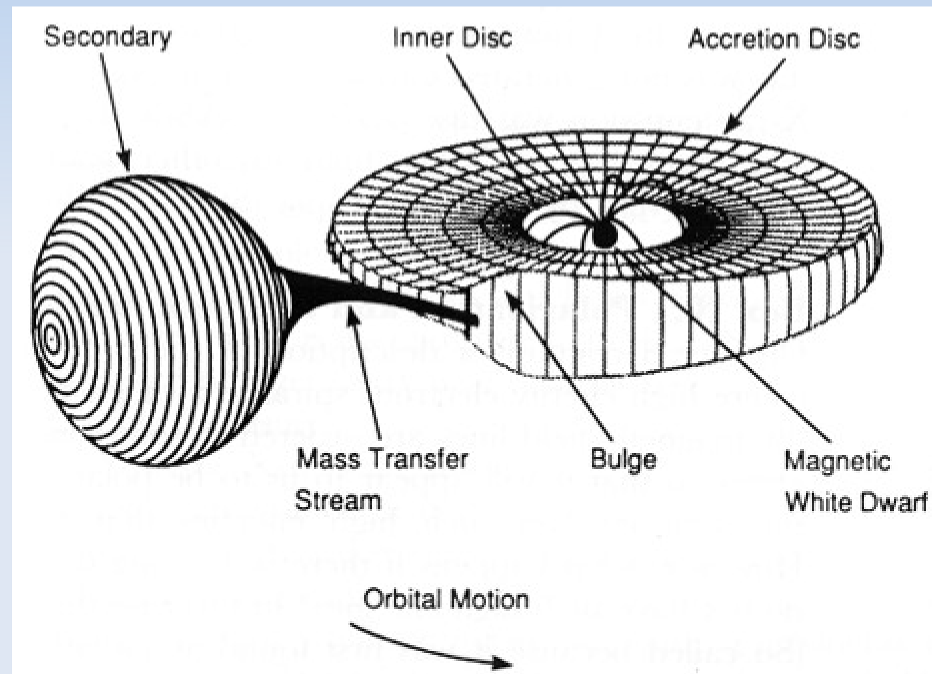

Spectroscopic analysis indicated the system consisted of a white dwarf of about 1.2 times as massive as the Sun, with an accretion disk, and a companion star with about 20% of the Sun's mass (Arenas et al. 2010). The two stars orbit each other approximately every 3 hours 20 minutes.[

Cataclysmic Variables

- Compact binaries
- White dwarf primary and Sun-like star secondary
- Several hundreds are known; classification based on history of observations
- They contain (classical) novae, supernovae (Ia), recurrent novae, dwarf novae, polars, intermediate polars...

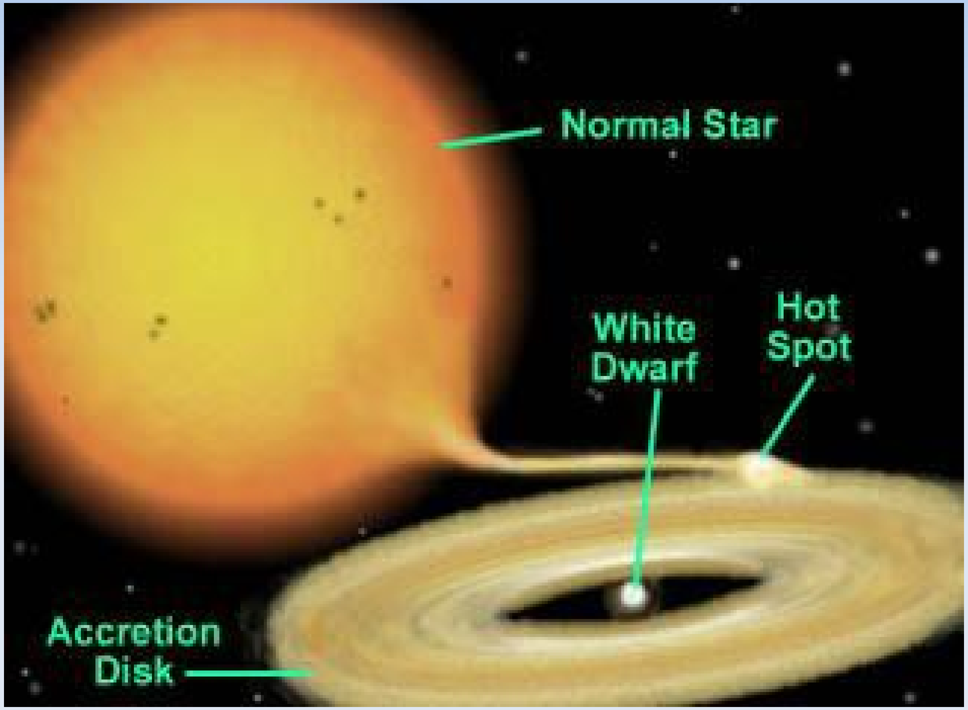

Cataclysmic Variables

- Based on long term variability we have
  - Classical Novae
  - Dwarf novae
- Classical Novae may be single or recurrent events (Δt=10-100 yrs)
- Based on short-term variability, features like superhumps on orbital timescale, variations due to WD spin period, QPOs, flickering, pulsations occur.

Dwarf nova

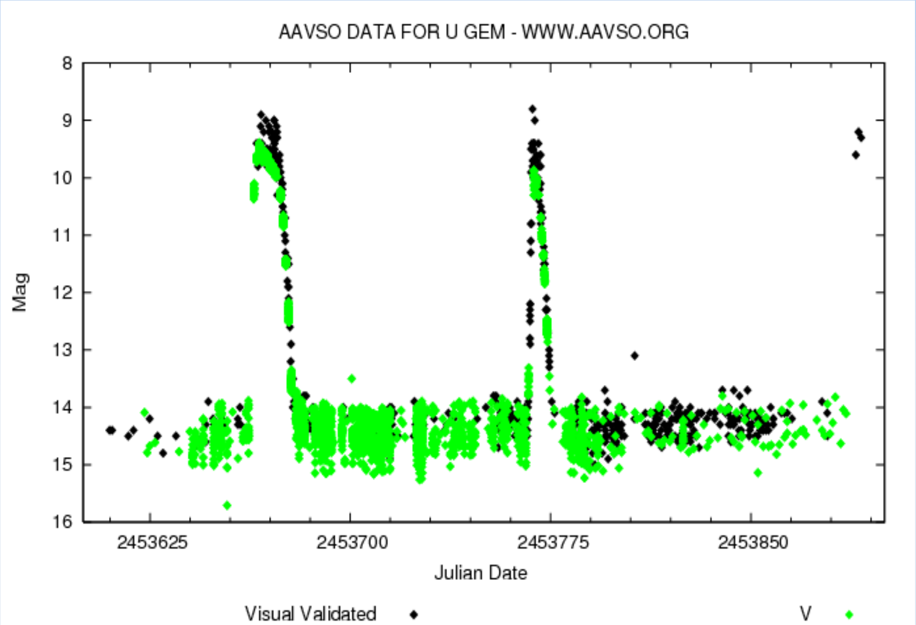

U Gem dwarf nova (outbursts every 100 days)

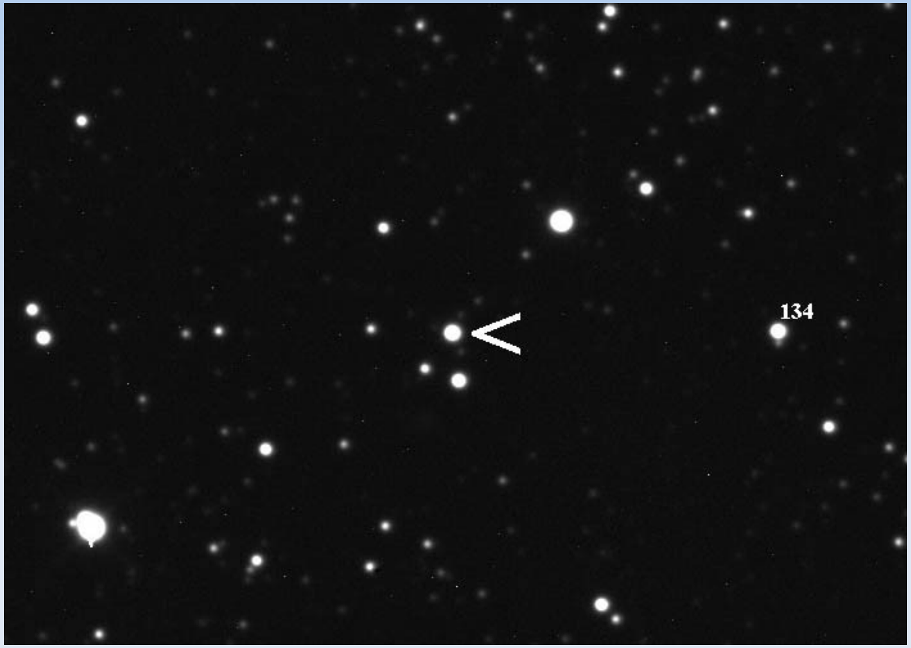

HT Cas dwarf nova (2010)

- U Gem, discovered in 1855, was initially thought to be a nova star.
- The mechanisms of outbursts for nova and dwarf nova are different!

SS Cygni

- Discovered in 1896
- Prototype of Dwarf Nova class
- Outbursts every 7-8 weeks, rising from +12 to +8 mag, in timescale of 2 days

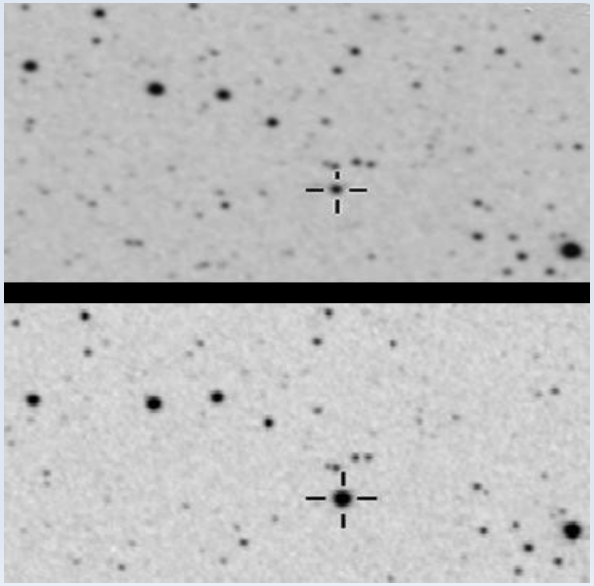

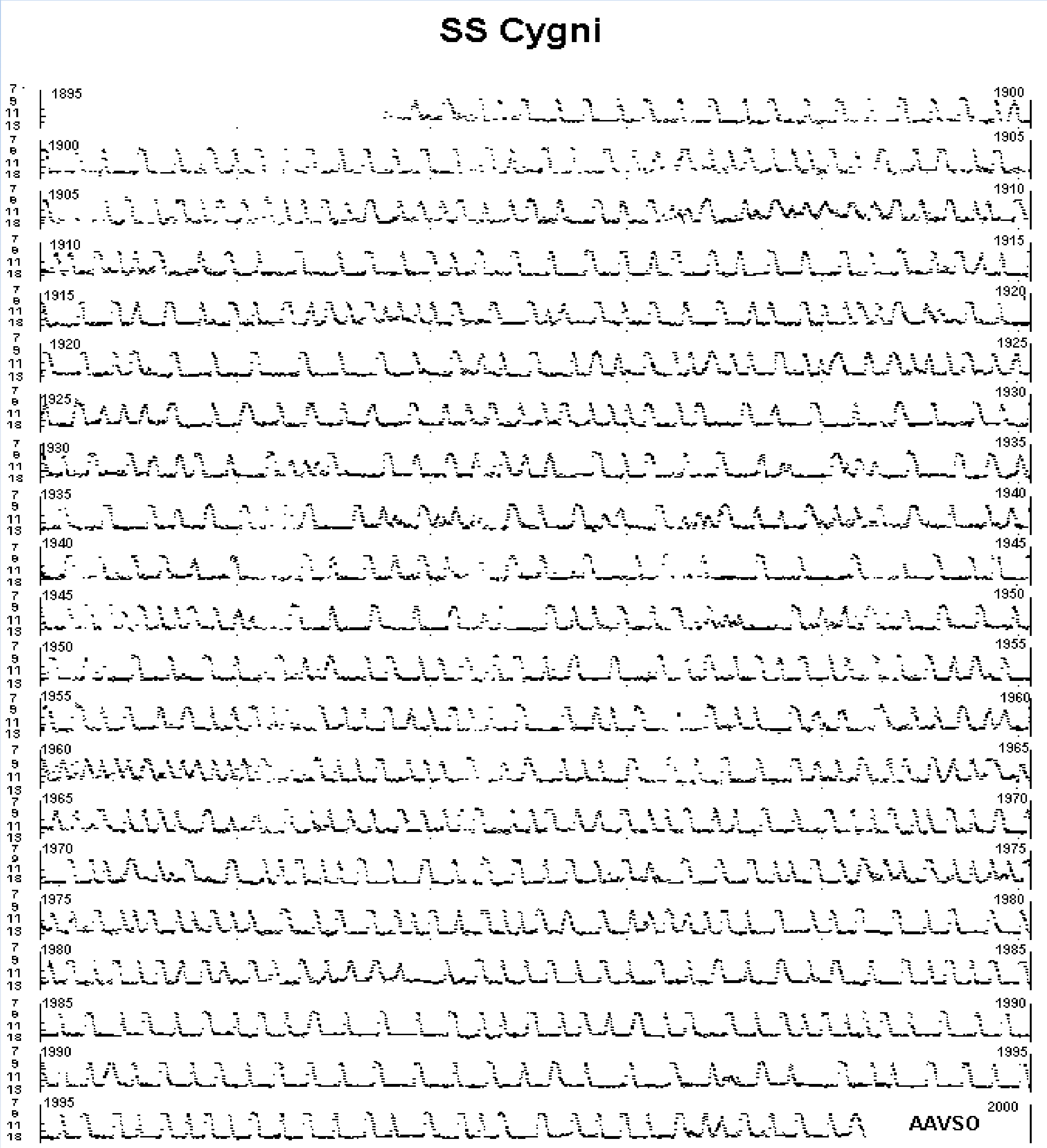

Dwarf Novae

- Eruptions are less violent than in novae (source brightens by 2-8 mag)
- Durations of outbursts are between 2-20 days. Intervals from 10 days to 10 yrs.
- Modeled as a temporary increase of mass acretion rate through the disk

Classes of DN

- SU Uma stars: exhibit outbursts and superoutbursts
- Z Cham stars: their outbursts cease sometimes, after maximum, for tens of days to years
- U Gem stars.

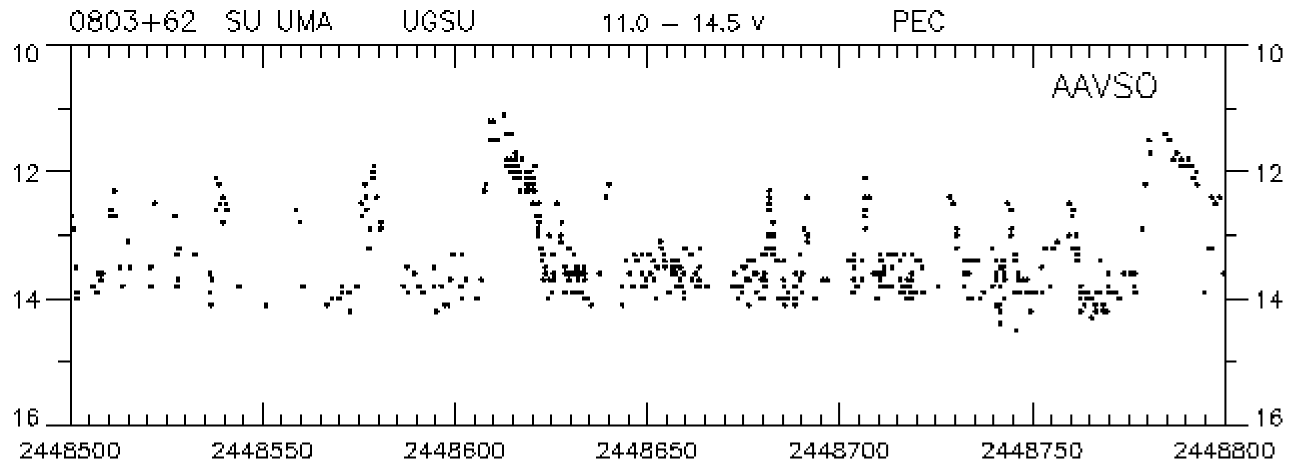

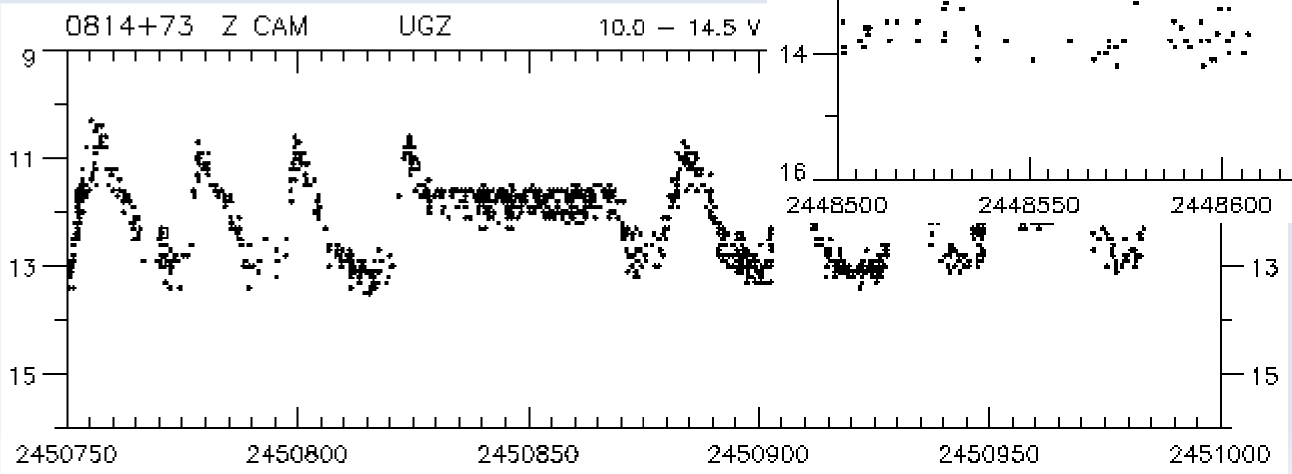

DN vs. CN

- During DN outbursts no shell ejection is observed
- Distinction between DN and classical (recurrent) novae is made spectroscopically

GK Persei: nova erupted in 1901

Cataclysmic Variables

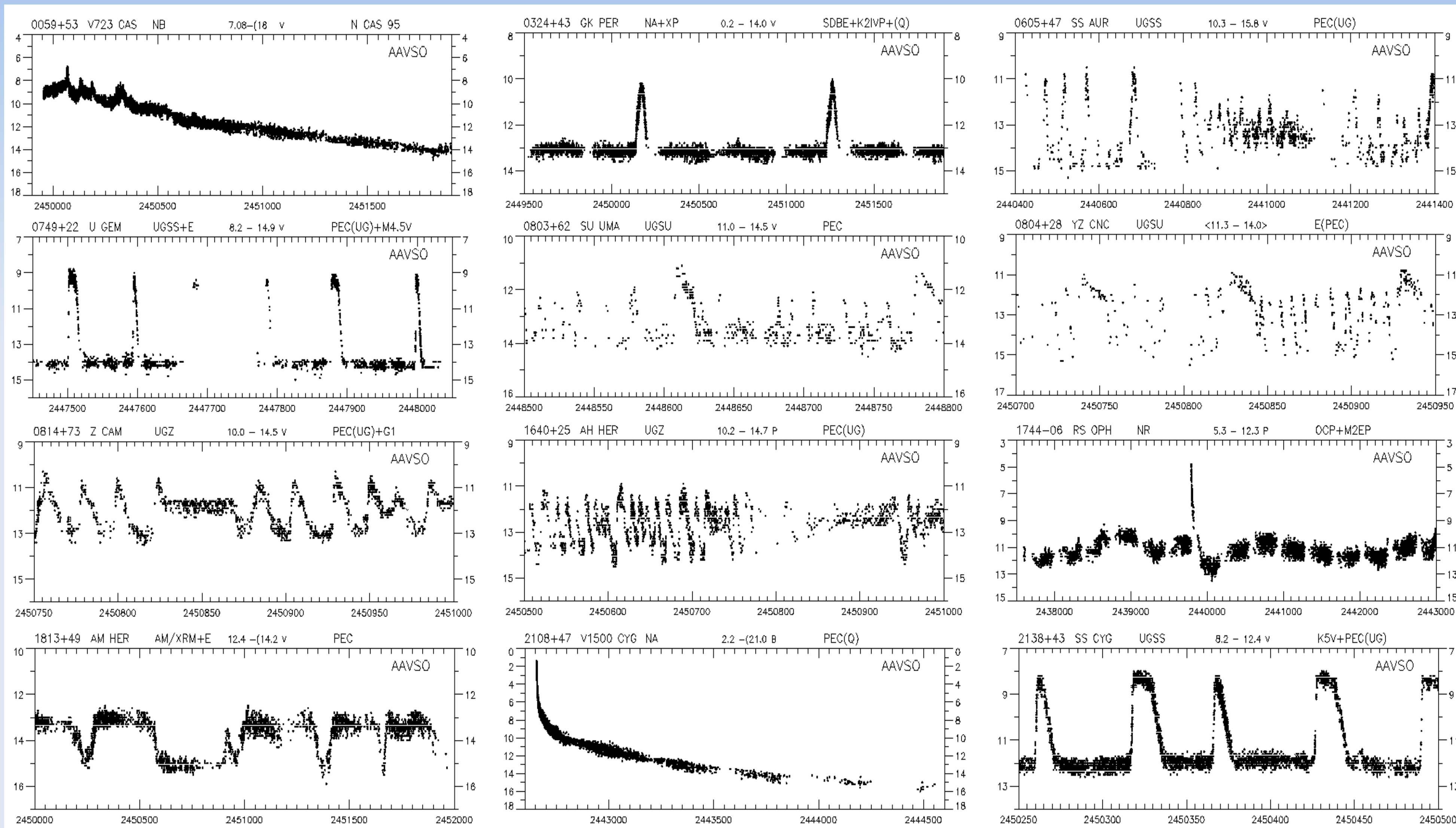

American Association of Variable Star Observers (AAVSO)

Recurrent novae

- The mass of white dwarf must be large (>1 M_{Sun}) and accretion rate high (> 10^{-7} M_{sun}/yr).
- The white dwarf may gain more mass between the eruptions, than it looses during ejections
- It may ultimately be the progenitor of a SN type Ia, when its mass exceeds the Chandrasekhar limit ($M_{Ch} \sim 1.4\ M_{sun}$)
- Nova remnant is made up of the material either left behind by the explosive fusion eruption (multiple ejections) by recurrent novae. Over their short lifetimes, nova shells show expansion velocities of around 1000 km/s, usually illuminated by their progenitor stars via light echos
- Known examples: T CrB, RS Oph, T Pyx, U Scor. The eruptions repeat every 20-80 yrs.

T Coronae Borealis

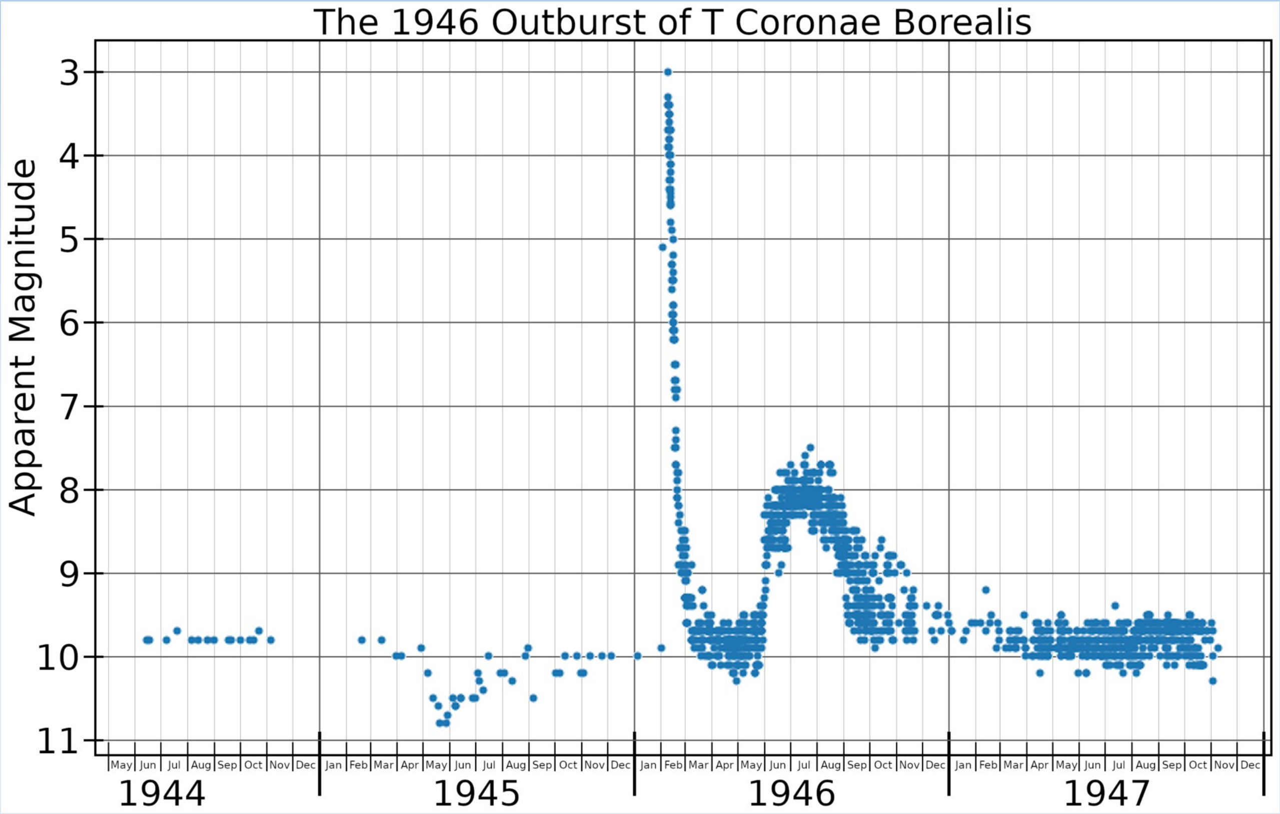

T CrB has been seen to outburst twice, reaching magnitude 2.0 on May 12, 1866 and magnitude 3.0 on February 9, 1946

X-ray Novae

- Analogous to dwarf nova, but compact star is neutron star or BH
- Outbursts on timescale of months, suggested also as dwarf-nova type (ionisation) instability (Lasota et al. 2001)

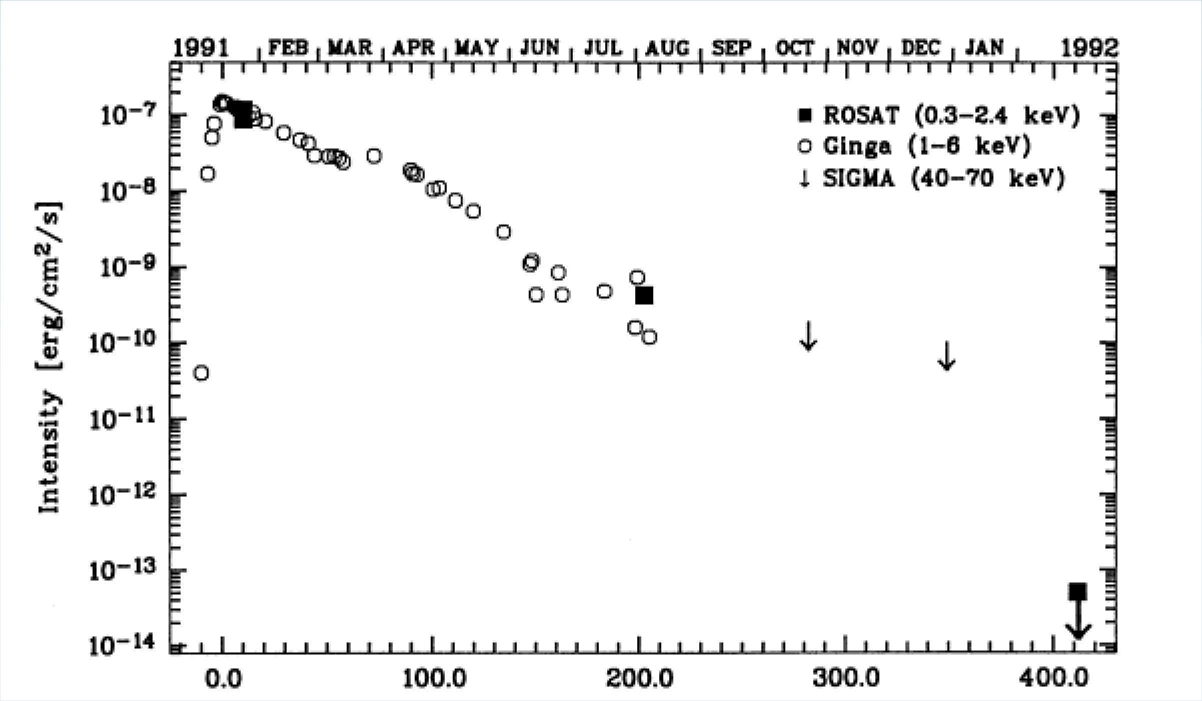

GRS 1124-683: Nova Muscae 1991 (Greiner et al. 1994)

X-ray novae

- Flux increase by 2-4 orders of magnitude in several days
- Decline time of ~ months
- Many of them are recurrent
- Possibly outbursts are due to accretion disk instability

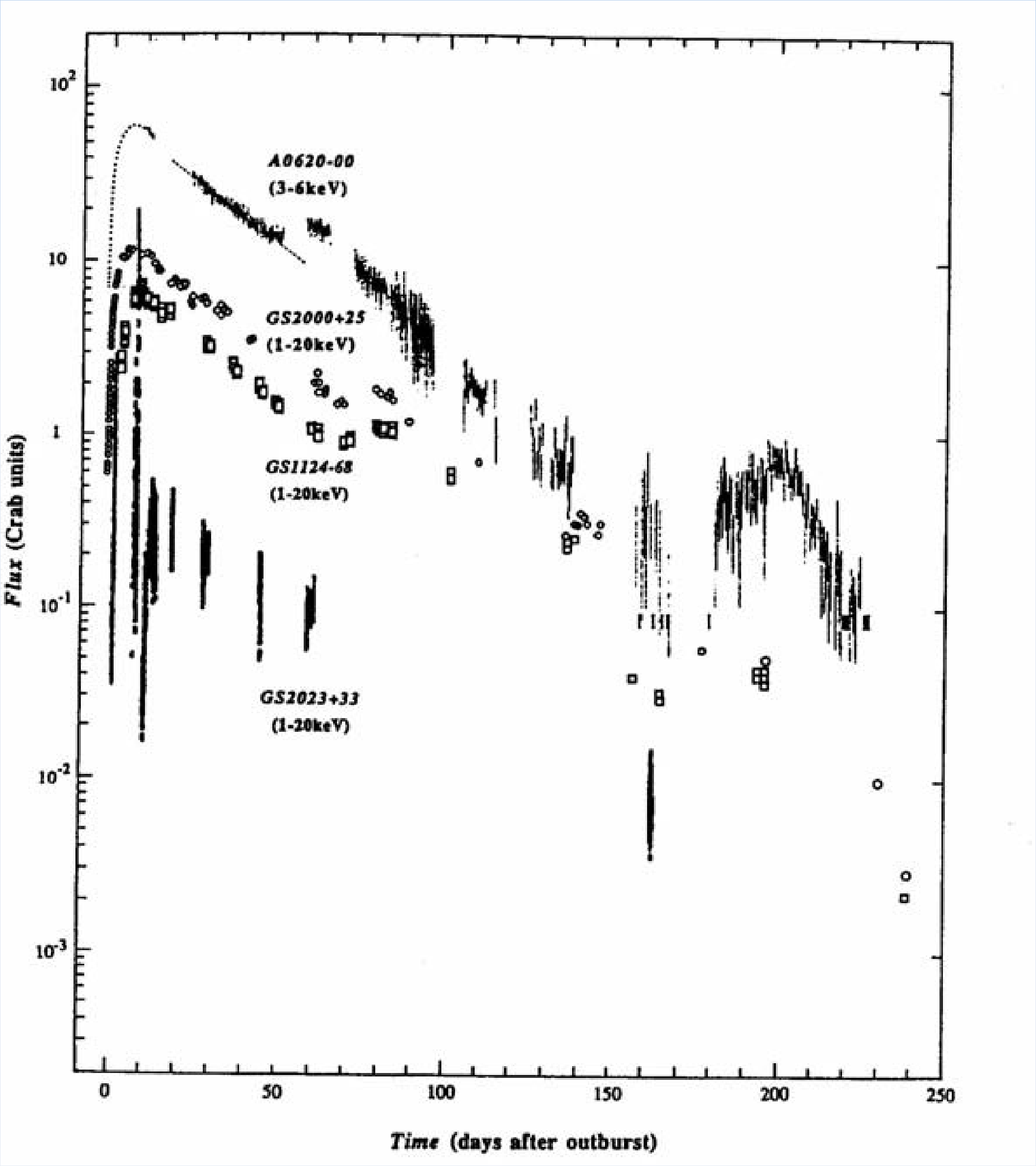

X-ray Novae

- Outburst mechanism may be analogous to dwarf nova, but compact star is neutron star or BH
- Outbursts on timescale of months, suggested also as dwarf-nova type (ionisation) instability (Lasota et al. 2001)

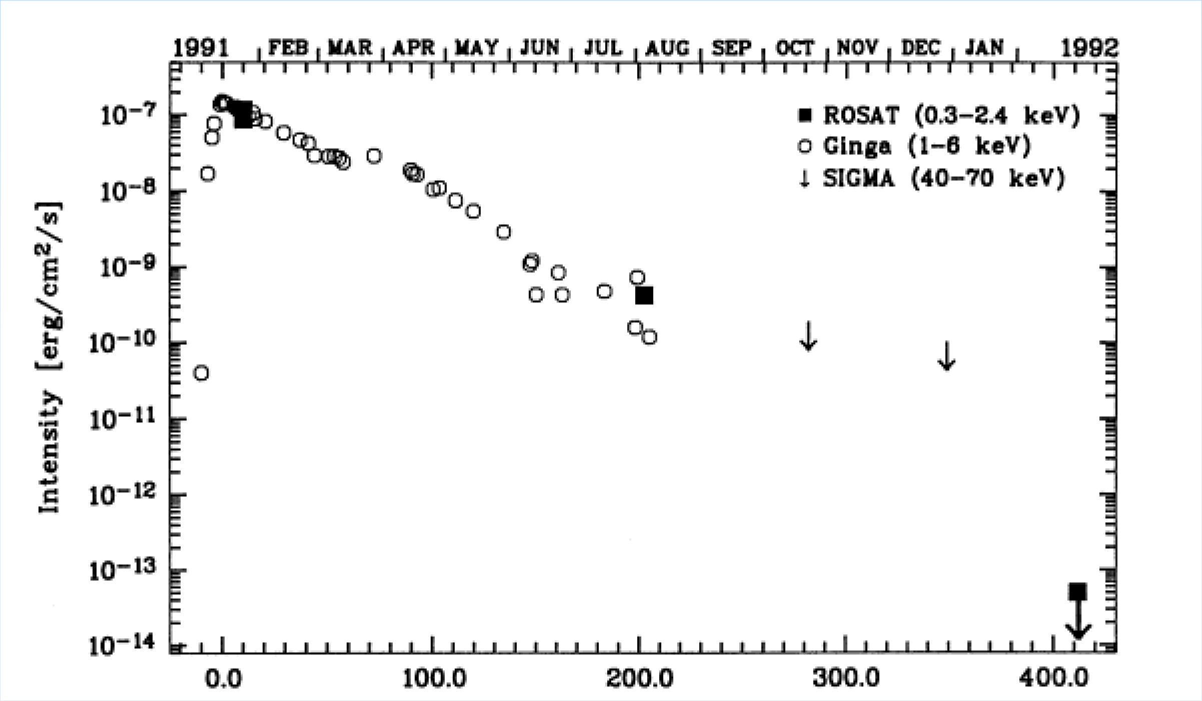

GRS 1124-683: Nova Muscae 1991 (Greiner et al. 1994)

What causes DN outbursts?

- Mass transfer rate from the secondary is constant. Mass is stored within the disk during quiescence, and suddenly accreted onto WD at some critical point, due to an unknown reason (Osaki 1971)
- Thermal instability of an accretion disk based on its bi-stable nature in temperature range of 10^3 - 10^4 K, when the Hydrogen changes from a neutral state to an ionized state
- Proposed by Mayer & Mayer-Hofmeister (1980) and Smak (1981)

Accretion disk instability

- Local solution of disk structure at radius R is represented by a point in the (density, temperature) plane
- Positive slope means stable solution
- Negative is unstable one

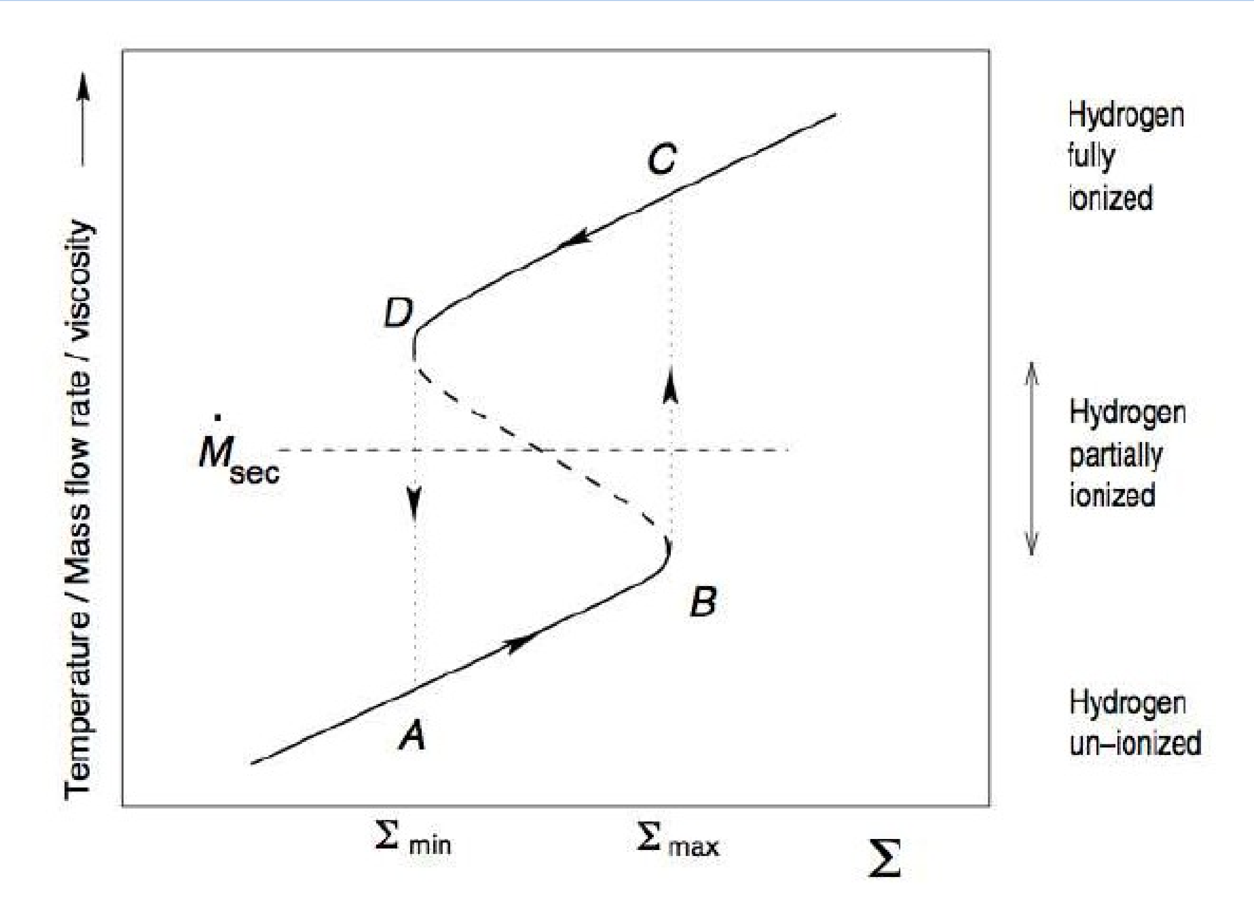

Opacities in the partial hydrogen ionization regime

- The Rosseland mean opacity due to atomic transitions, in the stable disk can be approximated by Kramers' law:

$$\kappa_R = 5\text{x}10^{24}\ \rho\ T_c^{-7/2}\ [\text{cm}^2\ \text{g}^{-1}]$$

- The electron-scattering opacity

$$\kappa_{es} = 0.2\ (1+X)\ \sim 0.34\ [\text{cm}^2\ \text{g}^{-1}]$$

dominates for an ionized gas, above $T>10^4$ K. Such temperatures would be obtained in steady disk solution at $R<R_{WD}$, unless accretion rate is very large.

- In general, the opacities are computed numerically and given in a form of tables (Cox & Steward 1965; Alexander et al. 1983)

Opacity dependence on temperature

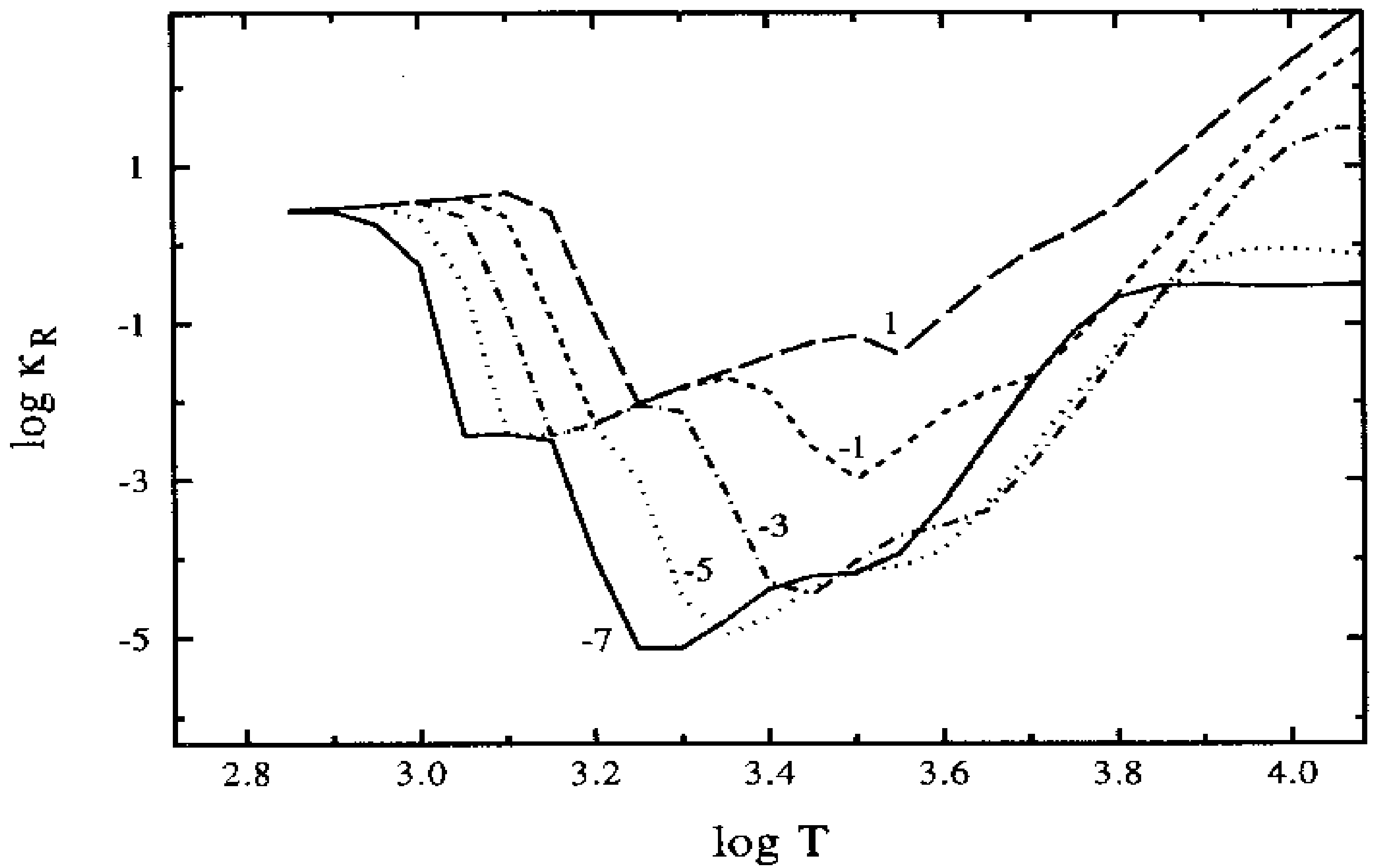

FIG. 2.—The Rosseland mean opacity as a function of temperature for the solar composition. Each curve is labeled with the value of log *R*.

From Alexander & Ferguson (1994). R is density ($R=\rho/T_6^3$)

Energy balance

- The vertically averaged heating due to viscous dissipation, according to SS73, is:

$$Q^{plus} = F_{visc} H = \frac{3}{2} \alpha P_{tot} \Omega H$$

- Cooling rate from radiative transport of energy:

$$Q^{minus} = F_{rad}(z = H) = \frac{4 \sigma T^4}{3 \kappa \rho H}$$

- Pressure (generally is a sum of gas and radiation):

$$P_{tot} = \frac{k}{\mu m_p} \rho T_c + \frac{4 \sigma}{3 c} T_c^4$$

Additional relations

- Hydrostatic equilibrium

$$\frac{P_{tot}}{\rho}=\Omega^2 H^2$$

- Total emitted flux

$$F_{tot}=\frac{3GM\dot{M}}{8\pi R^3}f(R)$$

- At high temperatures, gas is fully ionized. Free-free opacitiy processes are dominant, $\kappa=\kappa_{es}$=0.34.
- At lower temperatures, opacities are more complex and depend on density and T.

Break

Radial structure of accretion disk

- The mass conservation equation

$$R\frac{\partial \Sigma}{\partial t}+\frac{\partial}{\partial R}(R\Sigma V_R)=0$$

- Conservation of angular momentum

$$R\Sigma V_R\frac{\partial}{\partial R}\left(R^2\Omega\right)=-\frac{1}{2\pi}\frac{\partial G}{\partial R}$$

- Here V_R is the radial 'drift' velocity in the gas, and Ω is the (Keplerian) angular velocity. G(R,t) is the viscous torque, given by the kinematic viscosity and Ω'.

Radial structure

- Combining these two equations to eliminate V_R, we get the nonlinear diffusion equation:

$$\frac{\partial \Sigma}{\partial t} = \frac{3}{R} \frac{\partial}{\partial R} \left[R^{1/2} \frac{\partial}{\partial R} \left[\nu \Sigma R^{1/2} \right] \right]$$

and the radial velocity is given by

$$V_R = -\frac{3}{\Sigma R^{1/2}} \frac{\partial}{\partial R} \left[\nu \Sigma R^{1/2} \right]$$

- If ν is constant, then we can solve this by separation of variables, substituting $y=2R^{1/2}$

Spreading of a ring

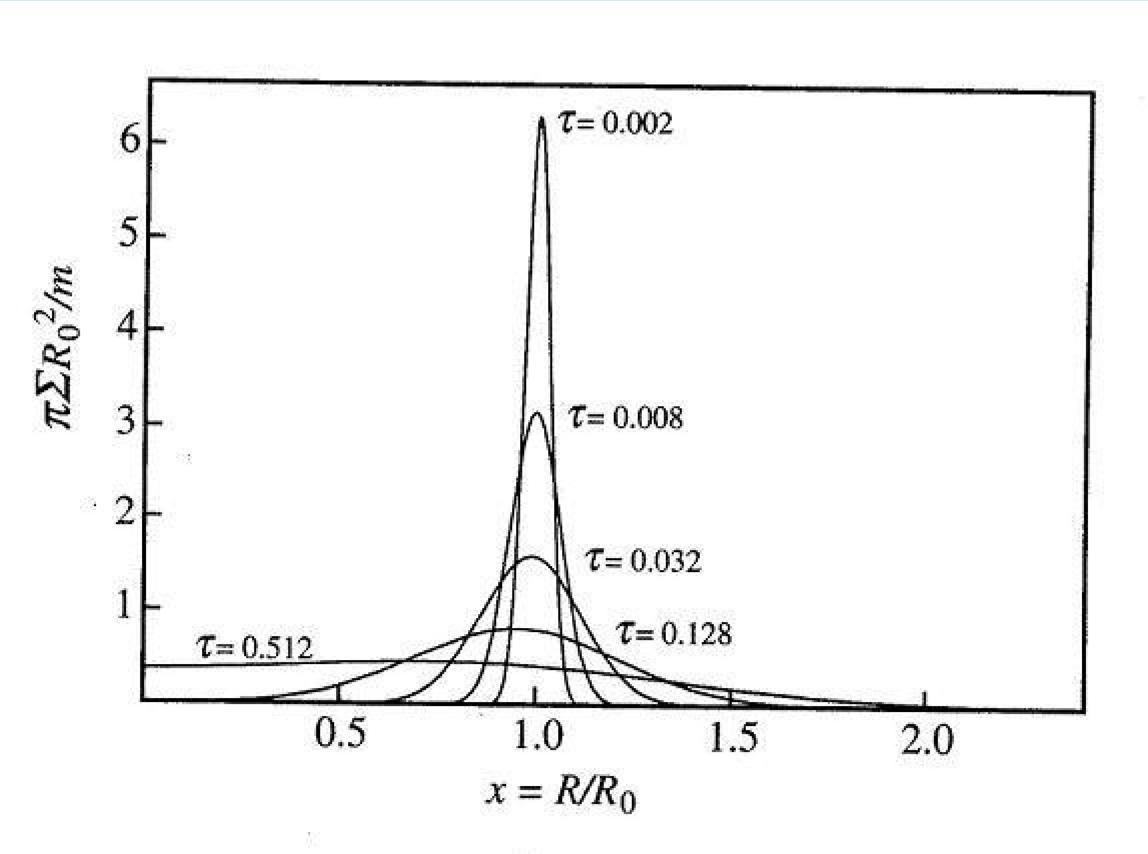

A ring of matter with mass m is initially placed in Keplerian orbit at R_0. Dimensionless time: $\tau = 12\,\nu\,t\,R_0^{-2}$

Viscous timescale

- Spreading of the original ring in radius occurs on typical timescale

$$t_{visc} \sim R^2/\nu \sim R/V_R$$

- The outer parts of disk move outwards, taking away the angular momentum of the inner parts, which move inwards, to the central star.
- After $t \gg t_{visc}$, almost all of the original mass will be accreted. All of the original angular momentum will be carried to very large radii, by a very small fraction of mass.

Characteristic timescales

- Viscous timescale – on which the matter diffuses through the disc under the viscous torque:

$$t_{visc} \approx \frac{R^2}{\nu} \approx \frac{R}{V_R} \approx \frac{1}{\alpha} \left(\frac{H}{R}\right)^{-2} t_{dyn}$$

- Dynamical timescale, on which small inhomogeniteis in the disk arise, and the hydrostatic equlibrium in the vertical direction is established:

$$t_{dyn} \approx \frac{R}{V_\phi} = \frac{1}{\Omega_K}$$

- Thermal timescale, over which the thermal equilibrium is adjusted. It is the ratio of heat content to the dissipation rate (per unit disk area):

$$t_{th} \sim 1/\alpha \; t_{dyn} << t_{visc}$$

Time-dependent equations

- To study full time dependence, we must allow for both evolution of density and temperature.
- We need to solve 2 differetial equations (diffusion and thermal imbalance), for Σ and T.
- Time does not appear explicitly on their right-hand side, so Σ and T span the phase-space.
- The stable fixed points are located on the Σ – T curves of positive slope. The negative slope branch contains unstable fixed points (limit cycle behaviour possible).

Thermal instability

- If the energy balance is disturbed in the disk, any instability will grow in t_{th}. The surface density may be fixed on this timescale.
- The vertical structure will respond to these changes on t_{dyn}, so it will be kept close to hydrostatic equilibrium.
- Instabilities arise when cooling rate Q^- can no longer cope with the heating rate $Q^+ \sim D$. When temperature T_c is increased by a small perturbation and Q^+ increases faster than Q^-, a steady state is impossible.
- Criterion: $\mathbf{d \log Q^- / d \log T_c < d \log Q^+ / d \log T_c}$

Viscous instability

- The disk on viscous timescale evolves much slower and maintains thermal and hydrostatic equilibrium
- Mass transfer rate depends on time at every radius, mass conservation equation is time dependent
- In diffusion equation, with $\mu = \nu\Sigma \sim$ Mdot $\sim$ T^4,

$$\frac{\partial}{\partial t}(\mu) = \frac{\partial \mu}{\partial \Sigma} \frac{3}{R} \frac{\partial}{\partial R}\left[R^{1/2} \frac{\partial}{\partial R}(R^{1/2}\mu)\right]$$

- If the coefficient is positive, then the perturbation will decay on the viscous timescale. For:

$$\frac{\partial \dot{M}}{\partial \Sigma} < 0$$

the local mass transfer rate will increase in response to decrease of density $\rightarrow$ matter will be removed from regions that are less dense

Time-dependent disk

- We have 2 differential equations (diffusion and thermal imbalance), for Σ and T.

$$\frac{\partial T}{\partial t} = Q^{plus} - Q^{minus}$$

$$\frac{\partial}{\partial t}(\mu) = \frac{\partial \mu}{\partial \Sigma} \frac{3}{R} \frac{\partial}{\partial R} [R^{1/2} \frac{\partial}{\partial R} (R^{1/2} \mu)]$$

- Instabilities arise when the volume cooling rate Q^- can no longer cope with the volume heating rate.
- $\mu = \nu\Sigma \sim$ Mdot $\sim T^4$. Instabilities arise when

$$\frac{\partial \dot{M}}{\partial \Sigma} < 0$$

Time dependent disk

- In alpha-disk, if the opacity in general is $\kappa \sim \rho T^{-n}$ the condition of viscous stability is broken for 7/2<n<13/2. This occurs in regions with T~6500 K, i.e. close to Hydrogen ionization temperature.
- Also, below T_H, if convective structure is considered, we expect inverse relation between T and Σ.
- The thermal balance condition also fails where dlogT/dlog Σ<0. The temperature may change:

$$\frac{\partial T}{\partial t} = Q^{plus} - Q^{minus}$$

A small perturbation will exaggerate thermal imbalance and disk is also thermally unstable.

Outburst modeling

- Outburst triggers at small R (inside -out propagation) or at large R (outside-in propagation), depending on global Mdot
- Heating wave switches disk to outburst
- Cooling wave switches disk to quiescence

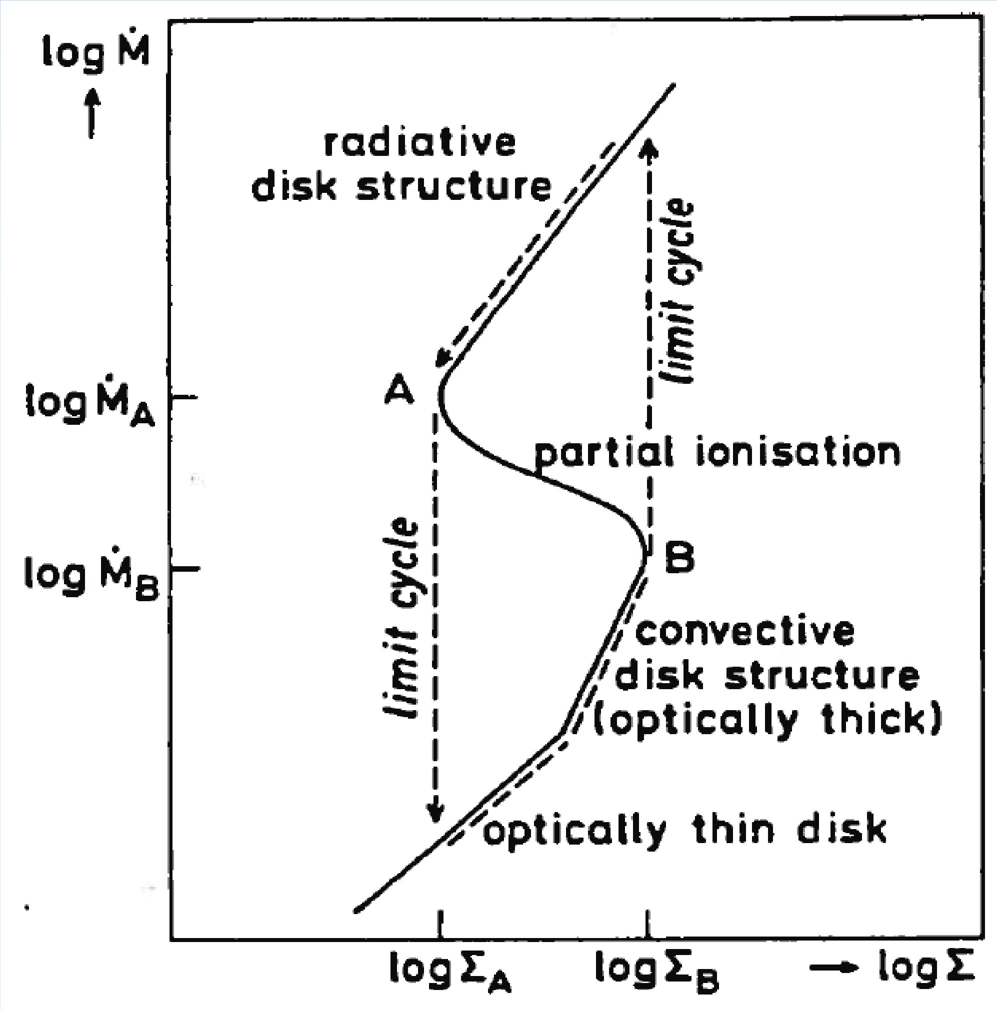

Outbursts modeling

- $M_{WD} = 0.6\ M_{Sun}$
- $\alpha_{hot} = 0.2$, $\alpha_{cold} = 0.04$
- Mean accretion rate Mdot = 10^{16} g/s (left)
- Mean accretion rate Mdot = 10^{17} g/s (right)

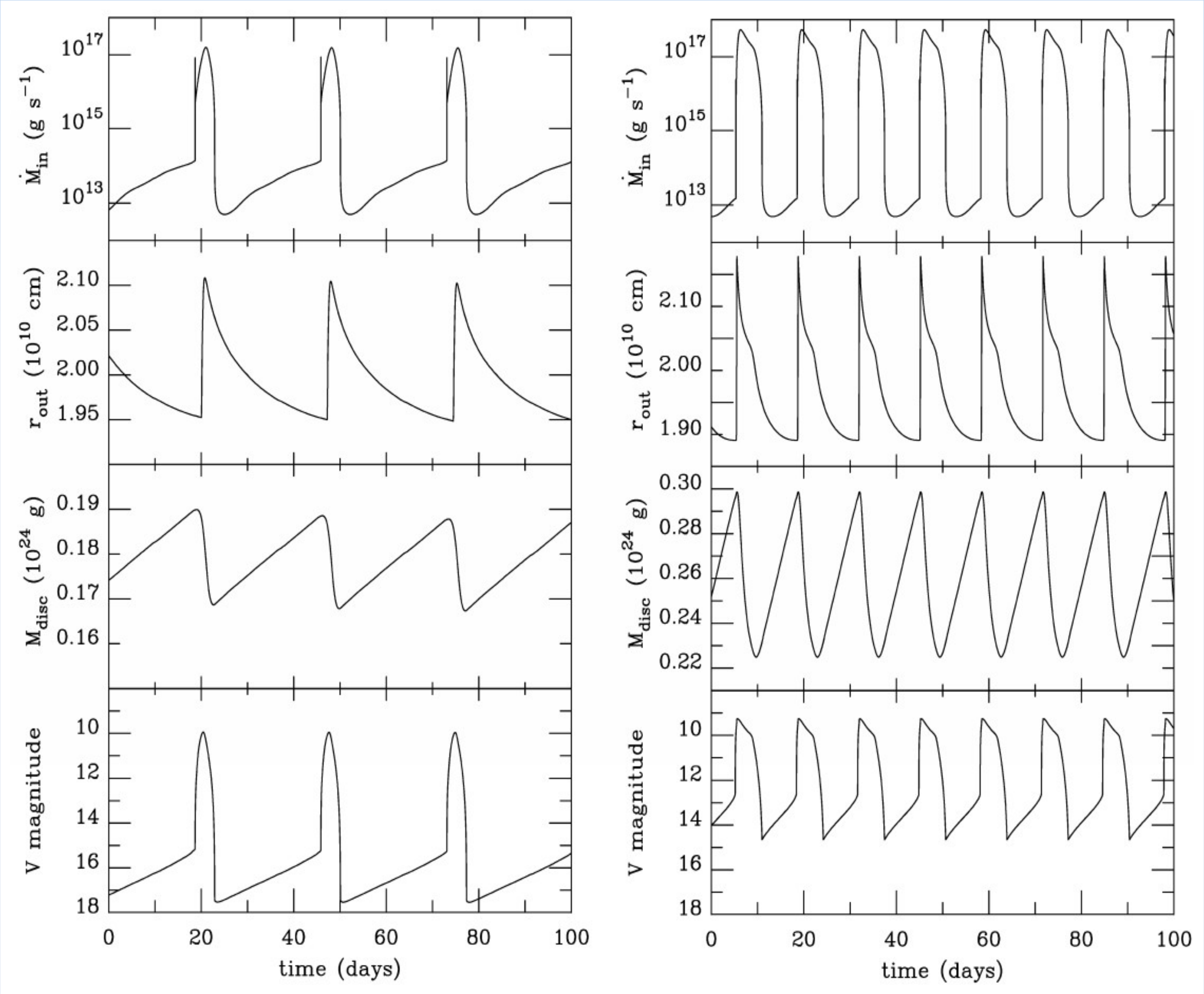

Hameury et al. (1998)

Two values of alpha

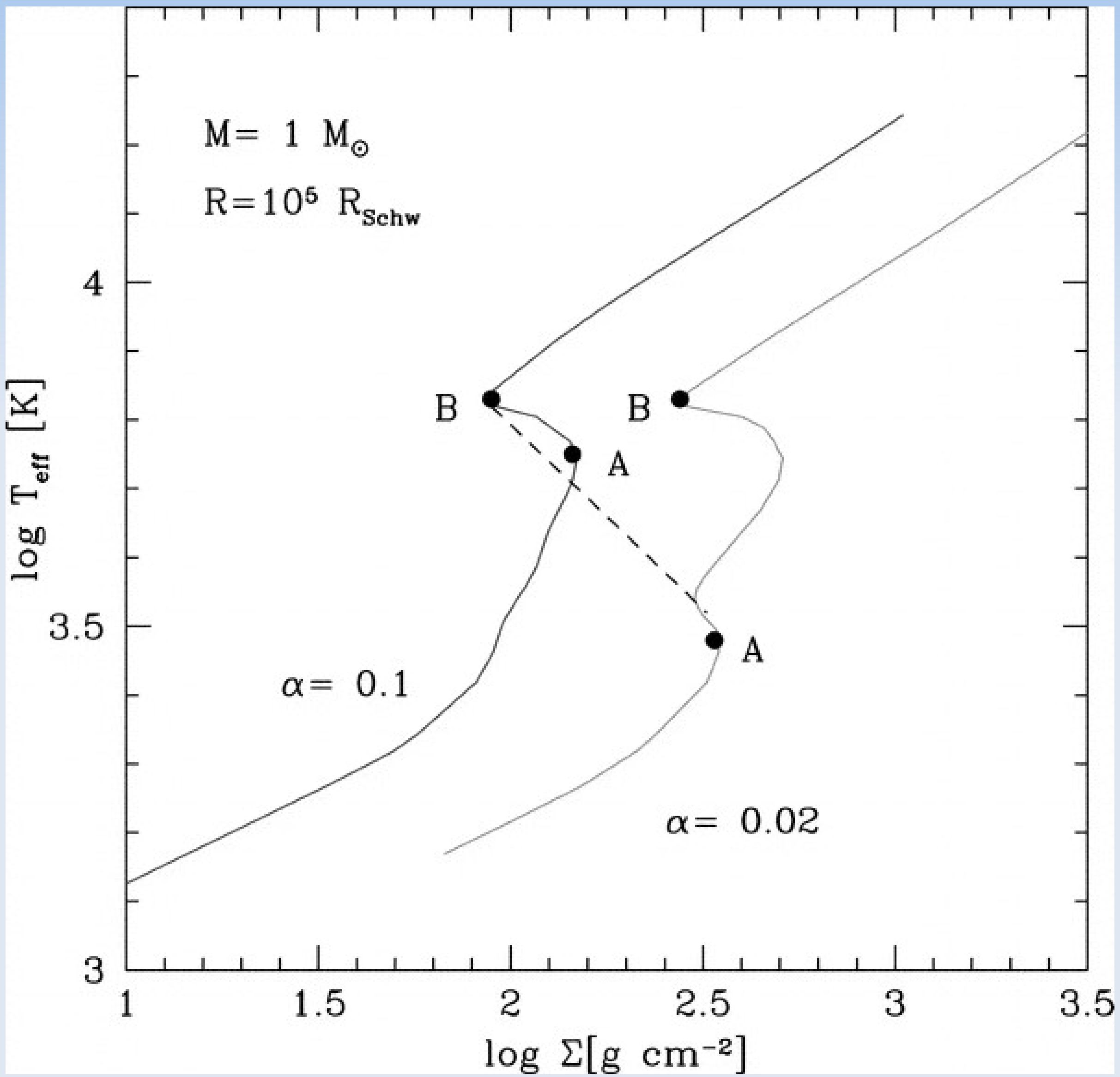

Janiuk et al. (2004, ApJ, 602, 595)

- Strength of the turbulences may be different in cold and hot states of the disk
- Hence two different values for viscosity parameter

Magnitude of viscosity

- For Keplerian disk, we have $\Omega' = (3/2)\,\Omega$ and from hydrostatic equlibrium, $c_s^2 = P/\rho = H^2\Omega^2$
- Therefore, the shear stress is $T_{r\phi} = 3/2\,\alpha\,P$ and viscosity magnitude can be estimated as

$$\alpha = 2/3\ T_{r\phi}/P$$

The stress computed in the shearing-box MHD simulations consists of Maxwell (magnetic) and Reynolds (turbulent) parts. Some numerical simulations show that consistent values of alpha are obtained with total pressure (Hirose et al. 2009; Jiang et al. 2013)

Magnitude of viscosity

- There is no reason to believe that viscosity is constant in time and throughout the disk.
- Probably, hydrodynamic mechanisms cannot produce sustained turbulence in differentially rotating disks
- Balbus & Hawley (1991) studied magnetorotational instabilities (MRI) and found they are effective in driving turbulences

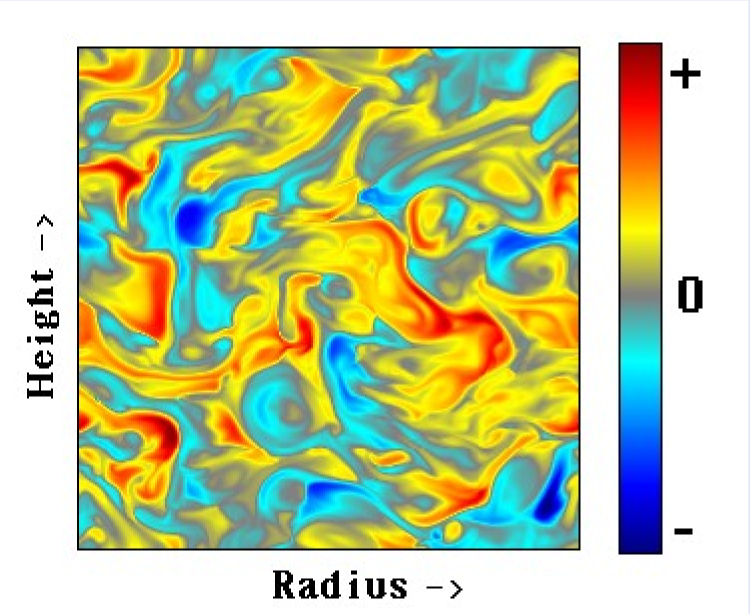

Superoutbursts, superhumps

- Modeled by the tidal instability of the outer disk
- Effects of disk ellipticity and precession
- 3:1 resonance with the orbital period
- Tidal-thermal instability model (Osaki 1989)

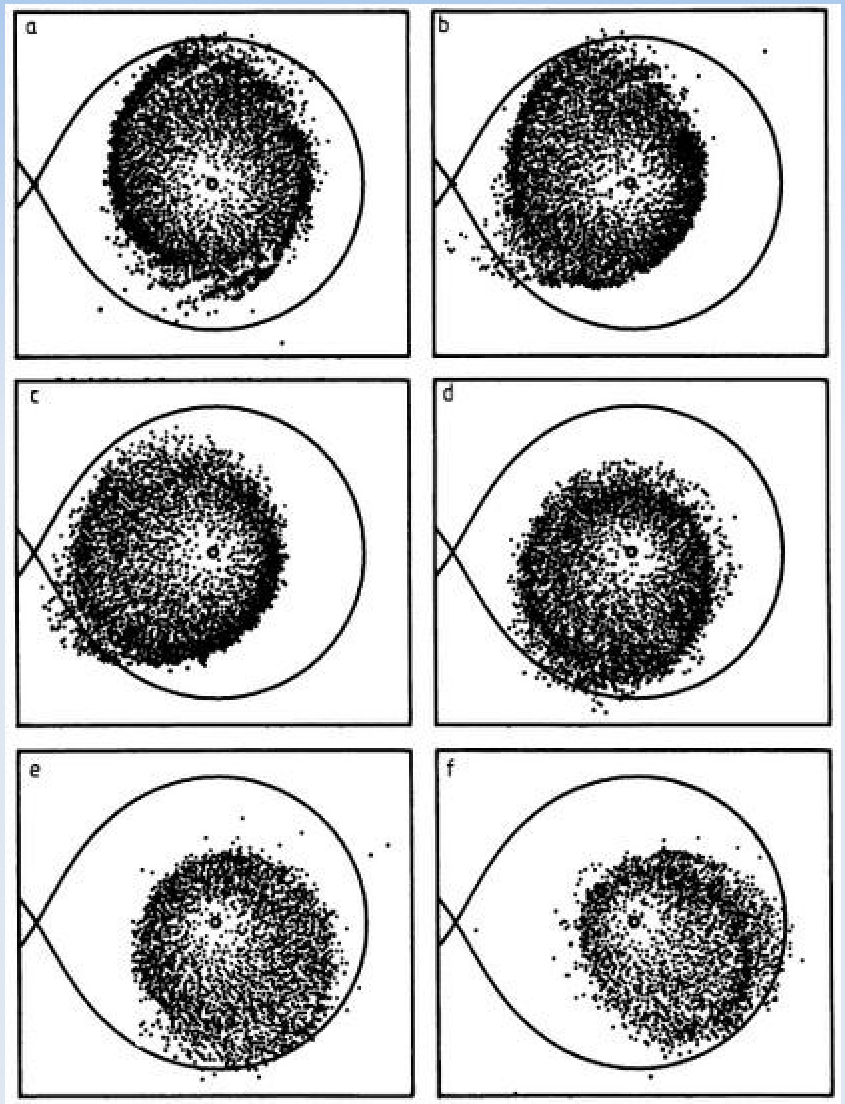

Thermal-visous limit cycle instabilities

- Another reason for thermal imbalance: radiation pressure

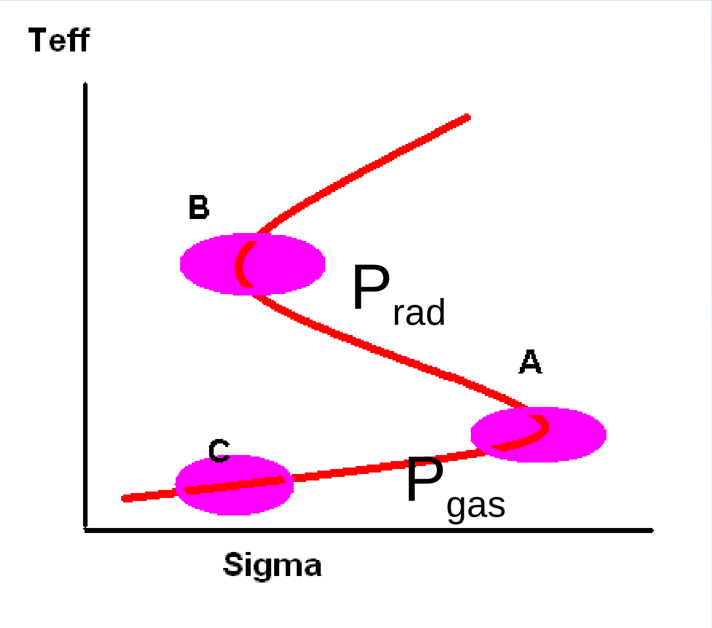

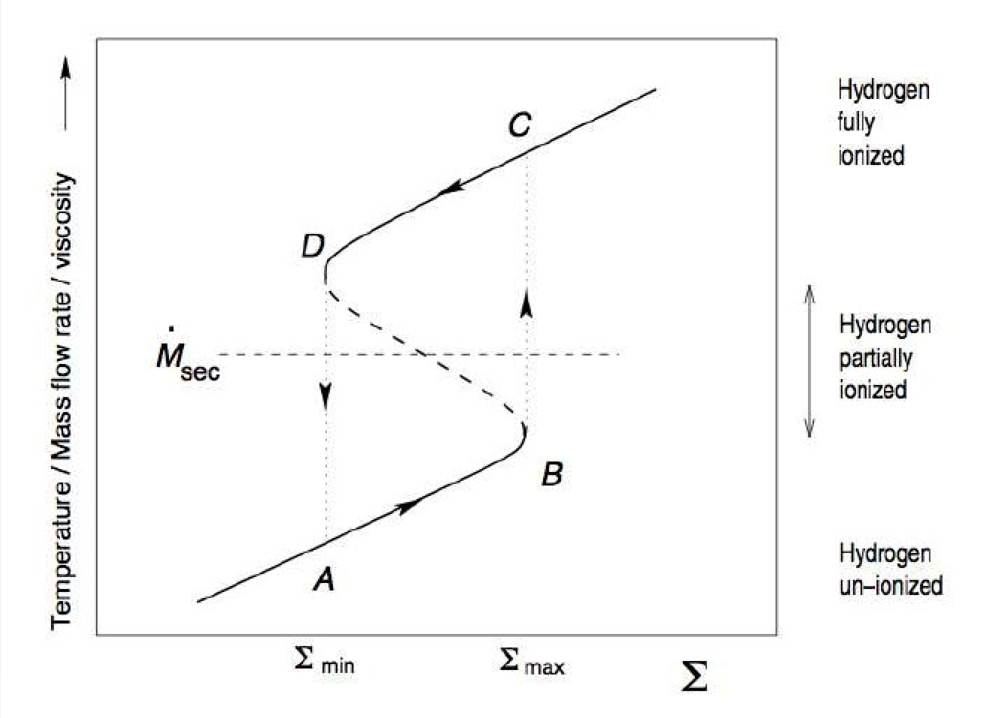

Note that in ionisation instability model (left plot), the disk was gas-pressure dominated, for all temperature range.
The radiation pressure starts dominating for temperatures higher than 10^6 K.

Stabilization of disk at high mdot

- Radiation pressure dominated disk was found unstable (Lightman & Eardley 1974), as $T \sim \Sigma^{-1/4}$.
- To have the limit-cycle type oscillations, we would need another, stable upper branch of solutions, with a positive slope.
- This is possible if additional cooling term in energy balance equation is introduced: advection.
- Thin disk approximation is not valid, as the accretion rate approaches Eddington limit.
- Practically, used is the 'slim disk' solution, with H/R~0.3 (Abramowicz et al. 1988).

Additional cooling: advection

- Black hole posses an event horizon instead of hard surface. This allows for accretion solutions in which significant fraction of dissipated energy is **advected** through the horizon instead of being radiated.
- Low radiative efficiency may occur in two cases:
  - Accretion rate is very small, gas has very low density and is unable to cool (*ADAF solution*)
  - Accretion rate and density is very high, flow is extremely optically thick, radiation is trapped and dragged down to the hole (*Slim disk solution*)

Advection

- The energy equation results from the net energy advection rate per unit volume,balanced by the volume heating and cooling rates:

$$q_{adv} = \rho V_R T \frac{dS}{dR} = q^{plus} - q^{minus}$$

- Here S is the specific entropy, q^+ is the viscous heating, and the cooling can be given by
- $q^- = n_e n_i \Lambda(T_e)$ (specified cooling function, optically thin case)
- or $q^- = \sigma\ T_{eff}^4\ /H$ (optically thick case, effective temperature at the surface).

Slim disk

- Disk is vertically integrated.
- Continuity and radial momentum equations satisfied
- Energy equation yields

$$Q_{adv} = \frac{\Sigma V_R}{R} T_c \frac{dS}{d \ln R} = \frac{\dot{M}}{2\pi R^2} c_s^2 \xi$$

where ξ is approximately a constant, on order of unity, weakly dependent on r.

- General slim disk solutions first given in Abramowicz et al. (1988)
- Luminosity of slim disk saturates due to advection, even for very large accretion rates (above Eddington rate).
- Full form of advective term, containing proper radial derivatives of temperature and density, for adiabatic gas with a given gas to radiation pressure ratio, can be found e.g. in Taam & Lin (1984)

Disk lightcurve model

- Dynamical model simulating the radiation pressure instability, with a slim disk closure
- Example plot for mean accretion rate Mdot = 0.7 $Mdot_{Edd}$, M_{BH} = 10 M_{sun}
- Code now is publicly available

https://github.com/agnieszkajaniuk/GLADIS

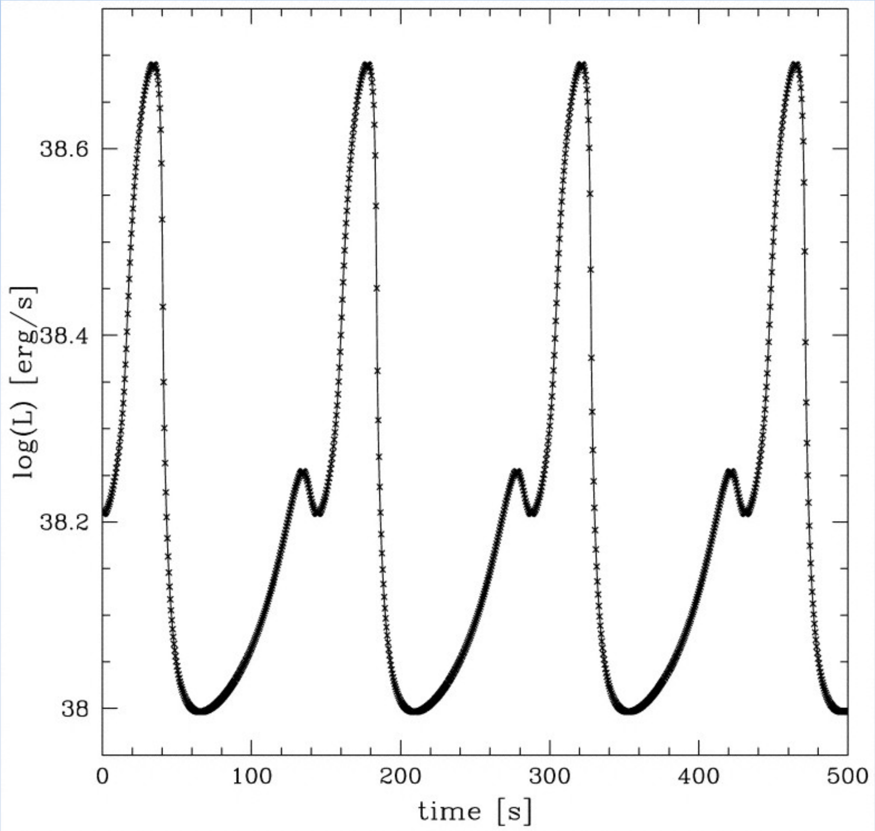

Janiuk, Siemiginowska & Czerny (2002)

IGR J 17091

- Micorquasar, observed since 1994
- In 2011 outburst it showed characteristic 'heartbeat states'
- Accretion rate about 25% of Eddington rate

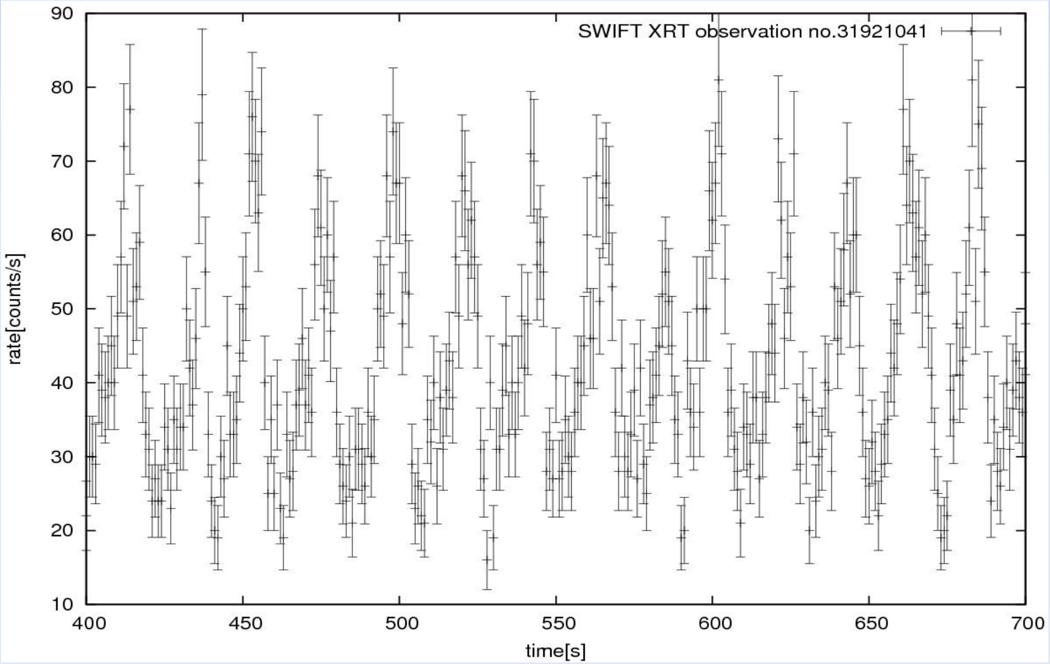

Janiuk et al.; 2015

Accretion disk instability simulation

- Simulation movie

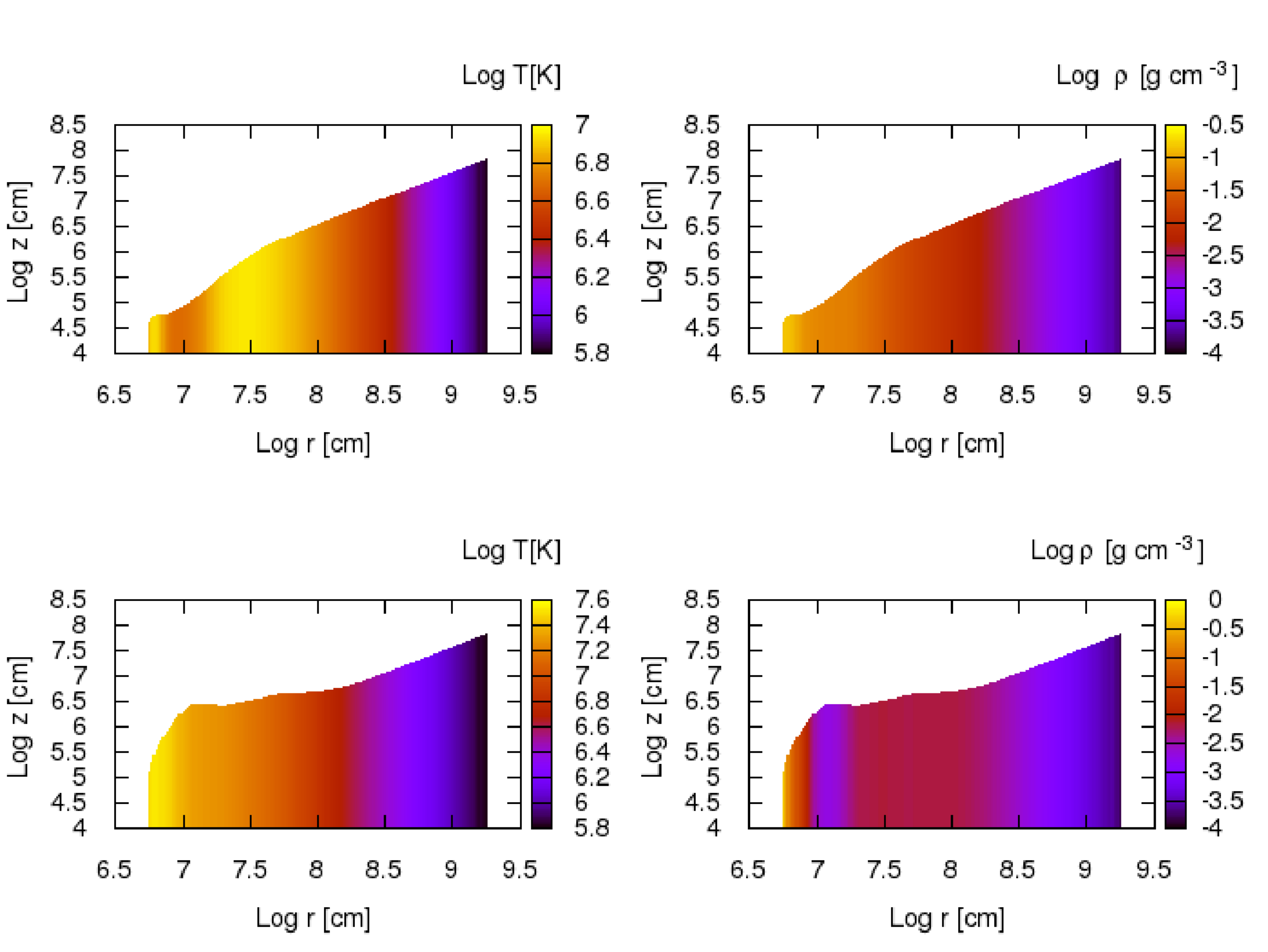

M. Grzędzielski et al. (2015)

Instability zones in the disk

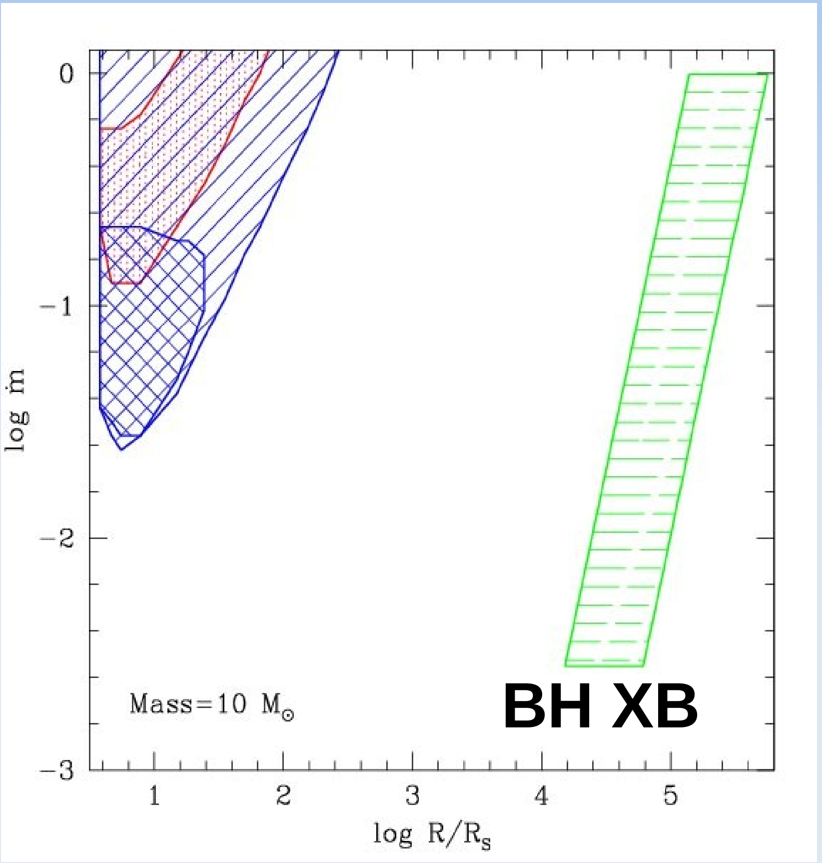

Extension of the instability zones, for a given mean accretion rate (in Eddington units).
Radiation pressure instability can be futher modified, if we account for alternative prescriptions for viscous stress tensor (blue: viscous heating due to total pressure; red: geometrical mean of gas and total pressure).

Plot from:
Janiuk & Czerny (2011)

Radiation pressure instability region is close to the inner edge in the disk. The hydrogen ionisation instability zone is much further out (green region), and may not appear if the disk is small.

Doubly-unstable sources

Table 1. Sample of the black hole X-ray binary sources. ΔT is the estimated duration of an outburst, and F_{max}/F_{min} is its amplitude. R_d/R_s is the estimated disc size in Schwarzschild units. The observations were found in the literature and taken from http://xte.mit.edu/

Source	ΔT	F_{max}/F_{min}	$\dot{M}/\dot{M}_{Edd}$	R_d/R_s	Instability	Ref.
A0620-00	150 days	300	$10^{-2}-3$	4.8×10^5	Ioniz.	14
GRS 1915+105	20-100 yrs	>100	0.25-0.7	6.3×10^5	Ioniz.	2
GRS 1915+105	100-2000 s	3-20	as above	as above	P_{rad}	1,3,19
GS 1354-64	~30 d	>20	0.1-1.8	1.8×10^5	Ioniz.	33
GS 1354-64	~20 s	1.5-2	as above	as above	P_{rad}	4,20,21, 35
XTE J1550-564	200 d	300	~0.15	1.3×10^5	Ioniz	36
XTE J1550-564	$\sim$2000 s	1.5	~0.15	as above	P_{rad}	5, 22
GX 339-4	100-400 days	75	<0.05	1.6×10^5	Ioniz.	6, 23, 24
GRO J0422+32	200 days	>30	$0.002-0.02$	4.8×10^4	Ioniz.	7, 25
GRO J1655-40	20-100 days	16	$5\times10^{-4}-0.45$	1.0×10^5	Ioniz.	8, 26, 27
GRO J1655-40	0.1-1000 s	7.5	as above	as above	P_{rad}	8, 32
4U 1543-47	50 days	300	$4.5\times10^{-4}-0.04$	9.6×10^4	Ioniz.	9
GS 1124-684	200 days	24	$\sim10^{-4}$ - ~1.0	5.2×10^4	Ioniz.	6,14
GS 2023+338	150 days	>100	$0.01-1.0$	3.8×10^5	Ioniz.	10, 29, 30
GS 2023+338	60 s ?	500	as above	as above	P_{rad}	10
SWIFT J1753.5-0127	150 days	10	0.03	2.0×10^4	Ioniz.	17, 31
4U 1630-472	50-300 days	60			Ioniz.	28
GRS 1730-312	6 days	200			Ioniz.	11
H 1743-322	60-200 days	100			Ioniz.	12
GS 2000+251	200 days	240			Ioniz.	6
MAXI J1659-152	20 days	15			Ioniz.	
CXOM31 J004253.1+411422	>30 days	>300			Ioniz.	13
XTE J1818-245	100 days	40			Ioniz.	15
XTE J1650-500	80 days	120			Ioniz.	16
XTE J1650-500	100 s	24			P_{rad}	18

[1] Wu et al. 2010; [2]Deegan et al. 2009; [3]Taam et al. 1997; [4] Revnivtsev et al. 2000;[5] Homan et al. 2001; [6] Tanaka & Shibazaki 1996; [7] van der Hooft et al. 1999; [8] Harmon et al. 1995; [9] Gliozzi et al. 2010; [10] in't Zand et al. 1992; [11] Trudolyubov et al. 1996; [12] Motta et al. 2010; [13] Garcia et al. 2010; [14] Esin et al. (2000); [15] Cadolle Bel et al. 2009; [16] Corbel et al. 2004,[17] Soleri et al. 2008; [18] Tomsick et al. 2003; [19] Belloni et al. 2000; [20] Kitamoto et al. 1990; [21] Casares et al. 2004; [22] Sobczak et al. 2000; [23] Hynes et al. 2003; [24] Miller et al. 2004; [25] Shrader et l. (1997); [26] van Paradijs 1996; [27] Kolb et al. 1997; [28] Buxton & Bailyn 2004 [29] Życki et al. 1997; [30] Życki et al. 1999; [31] Zhang et al. 2007; [32] Greiner 1994; [33] Brocksopp et al. 2001; [34] Osterbroek et al. 1997; [35] Cui et al. 1999; [36] Sobczak et al. 1999

Janiuk A. & Czerny B (2011)

Next week

- Microquasars.
- Astrophysical jets
- Some problems specific to disk accretion in Active Galactic Nuclei.

Further reading:

1) Alexander, D. R. & Ferguson, J. W. , *Low-temperature Rosseland Opacities,* Astrophysical Journal, vol. 437, p. 879-891 (1994)

2) Marigo P., et al., *Updated Low-temperature Gas Opacities with ÆSOPUS 2.0 ,* Astrophysical Journal, vol. 940, p. 129, (2022)

3) Balbus, S.A., Hawley, J.F., ApJ, 376, 214 (1991)